Julius-Maximilians-Universität Würzburg

Fakultät für Biologie

Combinational therapy of tumors in syngeneic mouse tumor models with oncolytic Vaccinia virus strains expressing IL-2 and INF-g. Human adipose tissue-derived stem cell mediated delivery of oncolytic Vaccinia virus

Dissertation

Zur Erlangung des naturwissenschaftlichen Doktorgrades der Julius-Maximilians-Universität Würzburg

vorgelegt von

Ivan Petrov

aus Novosibirsk, Russia

Würzburg, 2022

Submitted on: ……..……..

Member of the Promotionskomitee:

Chairperson: …… Prof. Dr. A. A. Szalay ……

Supervisor: ……Prof. Dr. T. Dandekar …….

Supervisor: ……Prof. Dr. U. Fischer…….

Date of public defense: ……..…

Date of receipt of certificates: …….…….

Parts of this thesis were first published in the following articles and a poster:

Petrov I, Gentschev I, Vyalkova A, Elashry MI, Klymiuk MC, Arnhold S, Szalay AA. **Canine Adipose-Derived Mesenchymal Stem Cells (cAdMSC) as a "Trojan Horse" in Vaccinia Virus Mediated Oncolytic Therapy against Canine Soft Tissue Sarcomas.** Viruses. 2020 Jul 12;12(7):750.

Draganov DD, Santidrian AF, Minev I, Nguyen D, Kilinc MO, Petrov I, Vyalkova A, Lander E, Berman M, Minev B, Szalay AA. **Delivery of oncolytic vaccinia virus by matched allogeneic stem cells overcomes critical innate and adaptive immune barriers.** J Transl Med. 2019 Mar 27;17(1):100. Erratum in: J Transl Med. 2021 Oct 4;19(1):414.

Petrov I, Szalay AA. "**Combinational therapy of tumors in syngeneic mouse tumor models with Vaccinia virus strains expressing IL-2 and INF-g**" Poster 024 at the 12th International Oncolytic Virus Conference, Rochester (MN, USA). 2019 Oct.

TABLE OF CONTENTS

SUMMARY

Cancer is one of the leading causes of death worldwide, with currently assessed chances to develop at least one cancer in a lifetime for about 20%. High cases rates and mortality require the development of new anticancer therapies and treatment strategies. Another important concern is toxicity normally associated with conventional therapy methods, such as chemo- and radiotherapy. Among many proposed antitumoral agents, oncolytic viruses are still one of the promising and fast-developing fields of research with almost a hundred studies published data on over 3000 patients since the beginning of the new millennia.

Among all oncolytic viruses, the Vaccinia virus is arguably one of the safest, with an extremely long and prominent history of use, since it was the one and only vaccine used in the Smallpox Eradication Program in the 1970s. Interestingly enough, it was the first oncolytic virus proven to have tumor tropism *in vitro* and *in vivo* in laboratory settings, and this year we can celebrate an unofficial 100th anniversary since the publication of the fact. While being highly immunogenic, Vaccinia virus DNA replication takes place in the cytoplasm of the infected cell, and virus genes never integrate into the host genome. Another advantage of using Vaccinia as an oncolytic agent is its high genome capacity, which allows inserting up to 25 kbps of exogenous genes, thus allowing to additionally arm the virus against the tumor.

Oncolytic virus action consists of two major parts: direct oncolysis and immune activation against the tumor, with the latter being the key to successful treatment. To this moment, preclinical research data are mostly generated in immunocompromised xenograft models, which have hurdles to be properly translated for clinical use. In the first part of the current study, fourteen different recombinant Vaccinia virus strains were tested in two different murine tumor cell lines and corresponding immunocompetent animal models. We found, that Copenhagen backbone Vaccinia

viruses while being extremely effective in cell culture, do not show significant oncolytic efficacy in animals. In contrast, several of the LIVP backbone viruses tested (specifically, IL-2 expressing ones) have little replication ability when compared to the Copenhagen strain, but are able to significantly delay tumor growth and prolong survival of the treated animals. We have also noted cytokine related toxicity of the animals to be mouse strain specific.

We have also tested the virus with the highest therapeutic benefit in combination with romidepsin and cyclophosphamide. While the combination with histone deacetylase inhibitor romidepsin did not result in therapeutic benefit in our settings, the addition of cyclophosphamide significantly improved the efficacy of the treatment, at the same time reducing cytokine-associated toxicity of the IL-2 expressing virus.

In the second part of the work, we analyzed the ability of adipose-derived mesenchymal stem cells to serve as a carrier for the oncolytic Vaccinia virus. We showed for the first time that the cells can be infected with the virus and can generate virus progeny. They are also able to survive for a substantially long time and, when injected into the bloodstream of tumor-bearing animals, produce the virus that is colonizing the tumor. Analysis of the systemic distribution of the cells after injection revealed that infected and uninfected cells are not distributed in the same manner, possibly suggesting that infected cells are getting recognized and cleared by an impaired immune system of athymic mice faster than non-infected cells. Despite this, injection of virus-loaded adipose-derived mesenchymal stem cells to human A549 tumor-bearing xenograft mice resulted in rapid tumor regression and reduced virus-related side effects of the treatment when compared to injection of the naked virus.

In conclusion, we have tested two different approaches to augmenting oncolytic Vaccinia virus therapy. First, the combination of recombinant Vaccinia virus expressing IL-2 and

cyclophosphamide showed promising results in a syngeneic mouse model, despite the low permissivity of murine cells to the virus. Second, we loaded the oncolytic Vaccinia virus into mesenchymal stem cells and have proven that they can potentially serve as a vehicle for the virus.

ZUSAMMENFASSUNG

Krebs ist eine der häufigsten Todesursachen weltweit, wobei die Wahrscheinlichkeit, im Laufe des Lebens an mindestens einer Krebsart zu erkranken, derzeit auf etwa 20 % geschätzt wird. Die hohen Fallzahlen und die hohe Sterblichkeit erfordern die Entwicklung neuer Krebstherapien und Behandlungsstrategien. Ein weiteres wichtiges Problem ist die Toxizität, die normalerweise mit konventionellen Behandlungsmethoden, wie Chemo- und Strahlentherapie, einhergeht. Unter den vielen vorgeschlagenen antitumoralen Wirkstoffen sind onkolytische Viren nach wie vor eines der vielversprechendsten und sich schnell entwickelnden Forschungsgebiete mit fast hundert veröffentlichten Studien an über 3000 Patienten seit Beginn des neuen Jahrtausends.

Unter allen onkolytischen Viren ist das Vaccinia Virus wohl eines der Sichersten und hat eine extrem lange und prominente Anwendungsgeschichte, da es der einzige Impfstoff war, der im Pockenausrottungsprogramm in den 1970er Jahren verwendet wurde. Interessanterweise war es das erste onkolytische Virus, dessen Tumortropismus in vitro und in vivo im Labor nachgewiesen wurde. In diesem Jahr (2022) können wir das inoffizielle 100-jährige Jubiläum seit der Veröffentlichung dieser Tatsache feiern. Obwohl Vaccinia hoch immunogen ist, findet die Replikation im Zytoplasma der infizierten Zelle statt, und die Virusgene werden niemals in das menschliche Genom integriert. Ein weiterer Vorteil der Verwendung von Vaccinia als onkolytisches Agens ist seine hohe Genomkapazität, die es ermöglicht, bis zu 25 kbit/s an exogenen Genen einzufügen, wodurch das Virus zusätzlich gegen den Tumor aufgerüstet werden kann.

Die Wirkung des onkolytischen Virus besteht aus zwei Hauptbestandteilen: der direkten Onkolyse und die Aktivierung des Immunsystems gegen den Tumor, wobei letztere der Schlüssel zum Behandlungserfolg ist. Bislang wurden präklinische Forschungsdaten meist in immungeschwächten Xenotransplantationsmodellen gewonnen, die sich nur schwer für den

klinischen Einsatz eignen. Im ersten Teil der aktuellen Studie wurden vierzehn verschiedene rekombinante Vaccinia-Virusstämme in zwei verschiedenen murinen Tumorzelllinien und in entsprechenden immunkompetenten Tiermodellen getestet. Wir fanden heraus, dass Kopenhagener Backbone-Vaccinia-Viren zwar in der Zellkultur äußerst wirksam sind, im Tiermodell jedoch keine signifikante onkolytische Wirksamkeit zeigen. Im Gegensatz dazu haben mehrere der getesteten LIVP-Backbone-Viren (insbesondere die IL-2 exprimierenden) im Vergleich zum Kopenhagener Stamm nur eine geringe Replikationsfähigkeit, sind aber in der Lage, das Tumorwachstum deutlich zu verzögern und das Überleben der behandelten Tiere zu verlängern. Wir haben auch festgestellt, dass die Zytokin-bedingte Toxizität der Tiere mausstammspezifisch ist.

Wir haben auch das Virus mit dem höchsten therapeutischen Nutzen in Kombination mit Romidepsin und Cyclophosphamid getestet. Während die Kombination mit dem Histon-Deacetylase-Inhibitor Romidepsin in unseren Versuchsreihen keinen therapeutischen Nutzen erbrachte, verbesserte die Zugabe von Cyclophosphamid die Wirksamkeit der Behandlung erheblich und verringerte gleichzeitig die zytokinbedingte Toxizität des IL-2-exprimierenden Virus.

Im zweiten Teil der Arbeit analysierten wir die Fähigkeit von aus Fettgewebe gewonnenen mesenchymalen Stammzellen, als Träger für das onkolytische Vaccinia-Virus zu dienen. Wir konnten zum ersten Mal zeigen, dass die Zellen mit dem Virus infiziert werden können und Virusnachkommen erzeugen können. Sie sind auch in der Lage, sehr lange zu überleben und, wenn sie in den Blutkreislauf von Tieren mit Tumoren injiziert werden, das Virus zu produzieren, das den Tumor besiedelt. Die Analyse der systemischen Verteilung der Zellen nach der Injektion ergab, dass infizierte und nicht infizierte Zellen nicht auf die gleiche Weise verteilt werden, was möglicherweise darauf hindeutet, dass infizierte Zellen von einem beeinträchtigten Immunsystem

der athymischen Mäuse schneller erkannt und beseitigt werden, als nicht infizierte Zellen. Trotzdem führte die Injektion von virusbeladenen mesenchymalen Stammzellen aus Fettgewebe in A549-Tumor-tragende Xenograft-Mäuse zu einer schnellen Tumorregression und zu geringeren virusbedingten Nebenwirkungen der Behandlung, als bei der Injektion des nackten Virus.

Zusammenfassend lässt sich sagen, dass wir zwei verschiedene Ansätze zur Verstärkung der onkolytischen Vaccinia-Virus-Therapie getestet haben. Erstens zeigte die Kombination aus rekombinantem Vaccinia-Virus, das IL-2 exprimiert, und Cyclophosphamid in einem syngenen Mausmodell vielversprechende Ergebnisse, trotz der geringen Permissivität der Mäusezellen für das Virus. Zweitens haben wir onkolytische Vaccinia-Viren in mesenchymale Stammzellen eingebracht und nachgewiesen, dass diese als Vehikel für das Virus dienen können.

CHAPTER 1: INTRODUCTION

1.1. Overview of cancer

According to International Agency for Research on Cancer (IARC), the current risk of developing cancer in a lifetime (before the age of 75) is about 20% [1]. The risk of dying from any type of cancer is 10%, meaning that approximately every fifth person will develop some form of cancer, and half of them will die from the disease. Advances in treatment strategies, development of new diagnostic tools, and their implementation as well as resulted in cancer-related deaths going down 27% in a period from 1999 to 2019 in the U.S., according to Centers for Disease Control and Prevention (CDC) report [2]. Another important factor brought up by the authors of the report is a population change in cancer risk factors, mainly cigarette smoking. The number of cigarette-smoking adults dropped from 42% in 1965 to 14% in 2019. However, cancer was still the second leading cause of death in the U.S. in 2019 and the positive changes in the country's cancer death rates may not reflect changes in worldwide cancer mortality. Thus, the development of new anticancer therapeutics and treatment strategies and translating them to clinics remains one of the key tasks for science and translational medicine. Amongst many new therapeutic approaches, oncolytic viruses remain one of the most promising tools in cancer therapy, which could also be confirmed by the number of recent and ongoing clinical studies. In the last twenty years, 97 studies have published data on 3233 cancer patients involved in clinical and preclinical trials of oncolytic viruses [3].

1.1.1. Cancer: tumor development, hallmarks of cancer

In 2000, Douglas Hanahan and Robert Weinberg put forward the theory of hallmarks of cancer, postulating that tumorigenesis is a somatic process, that begins from a single healthy cell that was able to accumulate enough aberrations to transform into a malignant cell [4]. The theory, which is

also known as somatic mutation theory, contains a description of six essential alterations acquired by tumor cells. According to it, a cancer cell is a cell that can self-sustain proliferative signaling, is not sensitive to growth suppressors, does not have a replication limit, and can evade apoptosis. On a tissue level, tumor cells can activate both invasions into adjacent tissues and the formation of distant metastases and induce angiogenesis. Based on remarkable progress in the research of tumor microenvironment (TME), Hanahan and Weinberg extended their theory 11 years later by adding two new, emerging hallmarks to the list – energy metabolism reprogramming and immune evasion [5]. They have underlined the importance of deregulation of energy metabolism of a tumor cell, thus enabling extensive cell growth and division, as well as the ability of solid tumors to avoid detection by various host immune system mechanisms.

Later the same year, Ana Soto and Carlos Sonnenschein proposed a theory of carcinogenesis called "the tissue organization field theory of cancer", opposing the prevalent somatic mutation theory of Hanahan and Weinberg [6]. In contrast to the somatic theory, Soto and Sonnenschein considered changes in physiological structure and function of tissue as two key factors of cancer formation and that cancer develops rather on a tissue level. The theory is quite well strengthened by practical evidence and validation difficulties of certain concepts of the somatic theory. To this date, a few attempts have been made to combine the theories, or to neglect one of them, but the problem of two different carcinogenesis theories based on the same experimental data remains unsolved [7–9].

1.1.2. Cancer: role of the immune system

Generally, the immune system is considered to consist of two parts, closely linked to each other and often overlapping: innate (general) immune system and adaptive (acquired, or specialized) immune system. All the functions of the immune system can be described by its major feature of

being able to distinguish “self” from “non-self”. It recognizes and neutralizes pathogens, foreign substances and normally fights arising malignant cells.

1.2.Vaccinia virus: introduction

Among all of the known viruses that possess certain oncolytic properties, the Vaccinia virus (VACV) remains one of the most appealing targets for implementing into wide clinical practice. VACV is a fast-replicating virus: the first viral particles are secreted from infected cells already after 6 hours post-infection [10]. Depending on the cell type, the majority of infected cells are being lysed approximately 48-72h after infection. Another advantage of VACV is the fact that it has an extremely wide range of tumors it can infect and replicate in, which might be explained by an unprecedentedly large group of viral proteins taking part in cell entry [11]. VACV genome has a remarkable cloning capacity: having a 200 kbp genome, the virus can be additionally armed with a reporter and therapeutic genes with up to 25 kbp of total length [12]. An important feature of the VACV replication cycle is the fact that it takes part exclusively in the cytoplasm of the cell, avoiding the possibility of a viral payload being integrated into the cell genome [13]. During its replication cycle, VACV produces a small percentage of distinctly structured infectious virions, called extracellular virus (EV) [14,15]. These viral particles incorporate several cellular membrane proteins that allow them to escape the host complement system and being able to spread to distant metastasis. Last but not least, the Vaccinia virus is probably the most comprehensively studied virus up to date, with the relative safety of its implementation confirmed by vaccination of hundreds of millions of people with different VACV strains during the Smallpox Eradication Program (1950-1980) [16].

1.2.1 Vaccinia virus: morphology and replication cycle

VACV is a large, double-stranded DNA, enveloped virus that belongs to the *Poxviridae* family. Its 190 kbp genome encodes more than 200 peptides [17]. VACV genes are classified as early, intermediate and late genes, with a few being expressed during the entire replication cycle [18–21].

Entry of Vaccinia virus into host cell cytoplasm is dependent on the host, virus strain, and virion form, and occurs by two independent mechanisms, either via a low-pH-dependent endocytosis or membrane fusion [22–24]. While EVs are presumably entering the cytoplasm by triggering the macropinocytic mechanism of endocytosis, mature virions (MVs) require a complex entry-fusion complex embedded into their membrane. Under certain conditions, VACV could even induce syncytia formation to facilitate virus transfer and amplification [25]. During the entry process, the virion loses its membrane or two membranes (in case of EV), and the core of the virion, consisting of viral DNA and shell formed by structural, transcriptional proteins and RNA, is transported into the cytoplasm via microtubules network [26].

The entire replication cycle of VACV takes place in specific regions of the cytoplasm, called virus factories, virosomes, or viroplasm, far from cellular organelles [27,28]. Viral RNA polymerase transcribes certain regions of viral DNA into mRNAs; newly translated viral proteins initiate replication of viral DNA and transform the entire cell machinery to serve virus needs and to mask it from host immune response. Newly formed viral particles are wrapped into membranes most likely derived from the endoplasmic reticulum [29,30]. Most of the newly formed infectious viral particles, MVs, remain in the infected cell, although in rare cases they are able to escape the cell, depending on VACV strain [31]. A small portion of structurally distinctive infectious virions, EVs, leave infected cells or remain attached to their membrane. While MVs are mostly responsible for host-to-host infection transfer, EVs are required for the virus to spread inside the host [32].

1.3. Immunotherapy of cancer: a historical perspective

The concept of immunotherapy was first described in the Ebers Papyrus (ci. 1550 BC). The Egyptian pharaoh Imhotep (2600 BC) recommended using poultice around tumor site followed by incision – resulting infection would cause tumor regression [33].

Spontaneous tumor regression is a rare, but well-documented phenomenon [34]. Although the most famous case, also known as St. Peregrine tumor, when a tibia tumor that required leg amputation suddenly disappeared, raises doubts about the lesion being malignant in the first place [35], virtually all other cases describe tumor regression concomitant with various infections.

During many centuries, this kind of "immunotherapy" went hand-to-hand with surgery treatment due to the lack of sterile conditions. Surgeons, while removing the tumor, would unavoidably contaminate the surgery site. In most cases, that would lead to sepsis, but rarely – help the patient fight residual tumor. Later, in the 17-19th centuries, several treatment strategies involved deliberately leaving the post-surgery wound open for a while, applying septic dressing to it, or even infecting it with syphilis, erysipelas, or gangrene [36].

In 1891, William Coley, a young surgeon at New York Memorial Hospital, found a peculiar sarcoma patient case in the hospital records. According to it, an immigrant patient with a sarcoma on his left cheek was operated twice but kept growing. Due to the size of the wound, it couldn't be closed, and led to erysipelas infection. The patient developed a high fever that couldn't be stopped, but his tumor began to shrink and finally completely disappeared. Coley found the patient and examined him. Seven years after the disease, there were no signs of tumor, but a large scar on the cheek [36]. Inspired by this, Coley infected ten of his patients with *Streptococcus pyogenes*, the bacteria, causing erysipelas, but struggled with consistency – in several patients it was hard to

induce the infection, in others the reaction was too strong, becoming fatal [37]. Coley decided to make a vaccine, a mix of two inactivated bacteria, *Streptococcus pyogenes* and *Serratia marcescens*, that would lead to inflammation and high fever avoiding the risks of an actual infection. The first case of using "Coley's toxins" was a man with inoperable sarcoma and resulted in complete remission [38]. Dr. William Coley can now be considered as the "Father of Immunotherapy".

Until 1892, when Dmitri Ivanovsky discovered the first known non-bacterial pathogen, known as the Tobacco mosaic virus, it was not clear if infectious diseases were caused by bacteria or viruses [39]. At the beginning of the 20th century, the first case reports of tumor remissions affiliated with viral infections were published, sometimes decades later the actual case, once the pathogenic agent became apparent [40,41].

The first report on using viruses for therapy of tumors was published already in 1912 by De Pace [42]. He was inspired by a case of cervical cancer patient remission after the patient had been vaccinated with rabies virus vaccine. De Pace inoculated eight cervical cancer patients with live-attenuated rabies vaccine and reported temporal remission and tumor shrinkage in several of them. [43]

In 1922, Levaditi and Nicolau were the first ones who showed viral oncolysis and tumor tropism of viruses in laboratory settings [44,45]. Interestingly, the object of their study was the Vaccinia virus. They observed that the virus is able to propagate in various mouse and rat tumors and could inhibit their growth.

Various wild-type viruses have been brought into early virus therapy studies in the 1940-1950s, including Hepatitis B, adenovirus, Mumps, and West Nile virus [46]. Despite sometimes

encouraging results, with several patients experiencing complete tumor regression, many of these studies lacked either efficacy or safety. At the same time, with radio- and chemotherapy slowly becoming a standard routine for cancer patients due to much better predictability of their therapeutical outcome and easier standardization procedure, the focus of cancer treatment shifted in an opposite direction. Contrarily to immune activation of the patient, introduced by Dr. William Coley, mainstream treatment strategies, such as radio- and chemotherapy, resulted in a suppression of the immune system of the patient making it that time harder to combine with the immune activation approach. With additionally arising barriers coming from the regulatory side, making it difficult to use living organisms for treatment, clinical studies of various pathogens for cancer treatment drastically decreased in their number in the 1970-1980s [46].

1.4. Tumor tropism of viruses

There are several mechanisms, that could contribute to the natural tropism of various viruses towards tumor tissue. It is known that newly generated vasculature in tumor tissue is usually hyperpermeable to macromolecules, possibly allowing viral particles to accumulate in tumor tissue in the first place [47,48]. Another reason why many viruses are selective towards the tumor could be explained by its altered energy metabolism, one of the hallmarks of cancer, proposed by Hanahan and Weinberg [5]. Viruses, not being a life form, have to rely on the metabolism of the host. Tumor cells are often described by their increased proliferation, thus becoming an attractive milieu for virus replication.

Another hallmark of cancer, immune evasion, largely contributes to viral tropism. While it is basically required for a tumor to build an immunosuppressive microenvironment to be formed, viruses might use it to their advantage to propagate inside the tumor tissue. Tumor cells often have

several defective regulatory pathways, such as IFN, Ras, PKR, p53, which don't let them easily shut down virus replication [49–51].

1.4.1 Mechanisms of action of OVs

The first mechanism of action is direct oncolysis: oncolytic viruses are able to infect cancer cells and associated endothelial cells and lyse them inside the TME. The second mechanism is eliciting an antitumor immune response, which starts immediately after the lysis. The lysed virus-infected tumor cells release not only new virus progeny, but also a large number of tumor antigens (TAAs) that are later phagocytized and can be presented by antigen-presenting cells (APCs), that in turn induce antitumor T cell response, which is supposed to change the immunosuppressive status of TME, turning it "hot" and allowing the immune response to eliminate not only the primary tumor but also distant metastases [52].

1.4.2 Translational challenges

However, there are a few barriers that could prevent the clinical translation of OV therapy. One of them is the problem of the delivery of the virus to the tumor site. When administered intravenously, the virus not only has to overcome host immune barriers in the blood, such as complement, coagulation factors, cell components, and neutralizing antibodies (nAbs) in case of pre-existing immunity but also be able to infiltrate the tumor. Dense extracellular matrix (ECM), together with abnormal microvascular and lymphatic vessel structure, results in interstitial hypertension of the majority of solid tumors and might drastically reduce tumor colonization by the virus [53,54]. Due to the abnormality of tumor vasculature, the TME is also known to be hypoxic, which not only promotes tumor growth, makes the tumors resistant to radio- and chemotherapy, but may also

reduce replication of certain viruses [55,56]. It is worth mentioning here that Vaccinia and several other oncolytic viruses may benefit from the hypoxic status of the tumor [57].

Heterogeneity of TME is another hurdle of oncolytic virus therapy. The APCs inside the TME might be inhibited by various immunosuppressive cell populations such as T-reg cells, tumor-associated macrophages, fibroblasts and neutrophils, and myeloid-derived suppressor cells [58]. Plenty of immune checkpoint inhibitors, such as PD-1/PD-L1 and CTLA-4, also contribute to the heterogeneity of the immunosuppressive status of the tumor. The ability of the virus to operate in these conditions and subsequently break them, turning a “cold” tumor into a “warm” one, is required for the success of the therapy.

Oncolytic viruses have to be highly immunogenic, and this is where another struggle of viral therapy comes from. OVs not only induce an antitumoral immune response but also a strong antiviral immunity, which might clear the virus from the tumor before the desired effect of the therapy takes place [59]. Finding the balance between the induction of tumor-specific immune response and limiting anti-viral immunity is a current task in the development of new OV treatment strategies.

1.5. Oncolytic viruses: modern history

Advances in genetic engineering, made in the 1980s, opened the opportunity to design more targeted and also armed oncolytic viruses. The attempts were made to overcome certain aspects of OV therapy, which led to a decrease in the number of cancer viral therapy clinical studies in the 1970s [46]. A deeper understanding of OV action mechanisms has also led to many combinational treatment strategies tested in preclinical and clinical trials.

1.5.1 Increased selectivity

Several strategies have been utilized to improve the ability of OVs to penetrate and home the tumor site. Unlike some viruses, such as Vaccinia, Vesicular stomatitis virus (VSV), and Herpes simplex virus (HSV) that can actually benefit from hypoxic conditions within the tumor, adenoviruses lose their replication and oncolytic efficiency in hypoxic settings [57]. To overcome this, Clarke designed a hypoxia-dependent adenovirus by setting the E1A gene of the virus under control of the hypoxia response element (HRE)-containing the promoter, [60]. The virus showed increased tumor selectivity and the ability to replicate in and destroy cancer cells in hypoxic conditions.

Complex ECM is another hurdle oncolytic viruses meet on the way to reach and lyse cancer cells. The approaches to break the ECM include pretreatment of the tumor with proteases or hyaluronidase or arming oncolytic viruses by encoding matrix metalloproteinases [61–64]. Interestingly, increasing cancer cell apoptosis also increases virus spread within the tumor, which has been shown by combinational therapy of the tumor with HSV and caspase-8 or paclitaxel [65]. Cytostatic-induced cell death resulted in a void space inside the tumor, which in turn promoted increased virus spread and oncolysis in a SCID mouse model.

The immunosuppressive environment inside the tumor might prevent OVs from generating an antitumor immune response, which is the key component of oncolytic virus therapy. In order to increase OV-driven alteration of TME, many viruses were armed with immunomodulatory agents, such as various cytokines or chemokines. Targeted expression of the payload inside the tumor could help to turn immunologically “cold” TME into a “warmer” state, providing recruitment of various immune cells to the site of virus-mediated inflammation or stopping the ones that are already presented in TME from supporting immune suppression. One of the most known examples of such a virus is talimogene laherparevec, an HSV expressing granulocyte-macrophage colony-

stimulating factor (GM-CSF) [66]. Expression of GM-CSF significantly enhanced release and presentation of TAAs and consequently – antitumor systemic immune response.

Immunomodulation can be achieved by arming OVs with cyto- or chemokines, for example, IL-2 or IFNg. The immunostimulatory effect of IL-2, a small protein that is mainly secreted by T helper cells, comes from its ability to activate a broad range of immune cells, such as lymphocytes, macrophages, and NK cells. Attempts to treat cancer patients with IL-2 began in the 1980s, but the application of the therapy was limited to the severity of side effects associated with it, mainly vascular leak syndrome (VLS) [67]. Nevertheless, these early applications of IL-2 are now considered to be the first effective immunotherapy for human cancer [68]. With an idea of limiting side effects by tumor-localized expression of IL-2, recombinant Vaccinia virus expressing either human or murine IL-2 was made and tested in both athymic and immunocompetent mouse models [69]. Systemic delivery of the virus armed with murine IL-2 resulted in preferential virus colonization of tumor and reduced tumor growth in 50% of the euthymic mice and complete rejection of tumor in 17% of the treated animals.

The idea of arming oncolytic viruses with IFNg is based on the ability of IFNg to upregulate MHCI expression, thus increasing antigen presentation on tumor cells and inducing a stronger immune response [70]. Interestingly, IFNg has also been shown to play a negative role when combined with oncolytic virus therapy. Its intratumoral expression upregulated expression of MHCII in GL261 tumor of C57Bl/6 mice, significantly decreasing permissivity of the cells to the virus [71].

Inducing immune response against the tumor by an oncolytic virus always goes hand-to-hand with identification and clearing of the virus itself by the patient's immune system. Altering the balance between antiviral and antitumoral immune response is another strategy to improve cancer therapy with OVs. This could be gained by many different approaches, including shielding of the virus

from both innate and adaptive humoral immune system achieved by carrier cells (MSCs, CAR-T cells, isolated tumor cells), by increasing EEV production (for Vaccinia virus), or by replacing the most nAbs-recognizable epitopes [72–76]. While there are many contradictions to the concept of suppressing the cell-mediated antiviral immune response, evading humoral immunity is undoubtedly a beneficial strategy to increase viral delivery in the case of systemic virus administration.

Modulation of cell-mediated antiviral immune response is hard to achieve without harming antitumoral immune activation. One of the possibilities is manipulation with the type I IFN pathway by a combination of oncolytic virotherapy with inhibitors of IFN response, such as ruxolitinib [77]. Many cancer types do not have a defective IFN pathway, which would cause resistance of the tumor to VSV replication much like it happens in healthy cells when VSV is injected alone. Combination with JAK/STAT inhibitor ruxolitinib significantly improves the therapeutical benefit of VSV treatment.

1.6. Romidepsin in treatment of cancer

Romidepsin is a histone deacetylase (HDAC) inhibitor obtained from *Chromobacterium violaceum* bacterium. It is inducing apoptosis in tumor cells by blocking HDAC and is approved by FDA for treatment of cutaneous and peripheral T-cell lymphomas. HDAC inhibitors are also known to be impairing the expression of interferons, thus increasing the cell permissivity to viruses [78]. This is one of the reasons that side effects of treatment with HDAC inhibitors, apart from nausea, vomiting, fatigue, and blood disorders, also include the susceptibility of the patient to various infections. Different oncolytic viruses, including VSV, HSV, adenoviruses, and Vaccinia have been tested in combination with different HDAC inhibitors [79]. When combined with the Vaccinia

virus, HDAC inhibitors increased viral replication and spread in both immunocompetent and athymic mouse models [80].

1.7. Cyclophosphamide

Cyclophosphamide (CPA) is a cell cycle nonspecific cytostatic agent, first synthesized in 1956 and approved for use in chemotherapy of cancer in 1959. It is a nitrogen mustard type alkylating agent, which activates in the liver by transforming into phosphoramide mustard. The cytotoxic effect of the metabolite is achieved due to cross-linking DNA and RNA, inhibiting protein synthesis. Treatment with CPA has a broad range of side effects including cardiotoxicity, infertility, suppression of the immune system, and even carcinogenesis. Interestingly, immune system suppression caused by CPA was found to be reversed by the addition of exogenous IL-2 [81]. Combination treatment with CPA and oncolytic Vaccinia virus has been shown to have synergistic effects in the xenograft lung adenocarcinoma model [82]. Co-treatment of PC14PE6 tumor-bearing mice with multiple injections of CPA (140 to 100 mg/kg) from day 0 to day 21 significantly increased virus spread and decreased blood vessel formation within the tumor.

1.8. ADSCs

ADSCs are mesenchymal stem cells (MSCs) obtained from fat tissue and are currently a hot spot of interest, mainly coming from the regenerative medicine field. The advantage of using ADSCs is their ability to migrate to the sites of inflammation, low immunogenicity, and high predictability, with only a few possible tissue-specific progenitors they can differentiate into. In contrast to bone marrow-derived mesenchymal stem cells, they are much more feasible to obtain with minimally invasive techniques.

Many studies point to the ability of mesenchymal stem cells to the home tumor site, including when they are loaded with an oncolytic virus [83–85]. For instance, when infected with measles and injected in SKOV3ip.1 orthotopic ovarian tumor-bearing mice, adipose-derived mesenchymal stem cells could protect the virus from nAbs, significantly prolonging survival of the animals when compared to treatment with the naked virus.

There is a debate currently going on, whether mesenchymal stem cells could themselves possess pro- or anti-cancer properties, or even become tumorigenic on their own [86]. Since the interaction mechanisms of MSCs with various immune cell populations within TME are not yet fully understood and could greatly vary from one tumor to another, the question remains unanswered. A few studies point out that MSCs can promote tumor growth by stimulation of blood vessel formation or release of various soluble factors that are further inhibiting immune response within TME [87,88]. Others suggest that MSC could be inhibiting tumor growth on its own by actually inhibiting angiogenesis and secretion of immunostimulatory factors inside the tumor [89,90]. In the end, pro- or antitumoral properties of MSCs seem to be mostly dependent on many factors, but mainly the cancer type.

CHAPTER 2: AIMS

Oncolytic viruses, in particular oncolytic Vaccinia virus, were of major growing interest during the past several past years, with a significant number of clinical studies going on in this field. However, there is a limited number of animal models, necessary preclinical data could be generated and most of them are hard to be properly translated into clinics. At the same time, one of the most crucial obstacles of oncolytic virus therapy is limited systemic delivery of the virus in a patient, when most of the virus can be cleared from the blood before it could reach the tumor.

The first goal of this work was to screen a panel of recombinant Vaccinia viruses for their ability to function in an immunocompetent mouse model. To evaluate the permissivity of murine tumors to the Vaccinia virus, we compared replication of fourteen different Vaccinia virus constructs in 4T1 murine breast carcinoma cells *in vitro* and designed an orthotopic tumor model to screen them *in vivo*. The most promising strain was then tested in combination with chemotherapy in another immunocompetent mouse model.

The second goal of this work was to evaluate the possibility of using human adipose-derived stem cells as carriers of the oncolytic Vaccinia virus. For a cell to be a functional virus carrier, it has to possess two key features: can migrate to the site of the tumor and be permissive to the virus infection. First, we wanted to evaluate the susceptibility of human adipose-derived stem cells to the oncolytic Vaccinia virus. Second, we designed an *in vivo* model to analyze the biodistribution of the cells and the virus and the effect of the virus-loaded stem cells on tumor growth.

CHAPTER 3: MATERIALS AND METHODS

3.1. Materials

3.1.1 Equipment

15 ml tubes (DB)

Accumet AR15 pH meter (Fisher Scientific)

Accuri C6 Flow Cytometer (BD Biosciences)

Anesthetic device (MSS)

Biofuge fresco Centrigufe (Heraeus)

Biomate 3 Spectrophotometer (Thermo Scientific)

BZ-X810 fluorescent microscope (Keyence)

Cell counting chamber (VWR)

Cell culture flasks (Corning)

Cell culture plates (Corning)

Cell culture plates (Sarstedt)

Cell scraper (Corning)

CFX96 Real-time System C1000 Touch (BioRad)

CK30 Inverted Phase Contrast Microscope (Olympus)

Class II Biological Safety Cabinet (HeraSafe)

CO2 incubator HERA cell 150i (Thermo Electron)

Cryo-tubes (Nalgene)

Cuvettes (Eppendorf)

Digital caliper (VWR)

EDTA tubes (DB)

Electrophoresis system (Bio-Rad)

ELISA plates (Costar)

EWJ precision balance (KERN)

GentleMACS Dissociator (Miltenyi Biotec)

In-vivo Fluorescence Imaging System (Maestro)

Lightpad A920 (Art Graph)

Mastercycler X50s (Eppendorf)

MEGA STAR Centrifuge (VWR)

Micro-Hematocrit Capillary Tubes (Global Scientific)

Microplate reader (TECAN)

Multichannel pipette (Integra Biosciences)

Orbital Shaker (VWR)

Pipet tips (VWR)

Pipettes (Eppendorf)

Realtime PCR (Bio-Rad)

Repeat dispenser (Eppendorf)

Rocking platform shaker (VWR)

Scalpers (Sklar instruments)

Sonifier 450 (Branson)

Stackable Incubator Shaker (New Brunswick Scientific)

Surgeon scissors (E.A Beck)

Syringes (DB)

TC-20 automated cell counter (Bio-Rad)

Transilluminator (PeqLab)

Tweezers (E.A Beck)

VX100 Vortex (Labnet)

Water bath (Fisher Scientific)

3.1.2. Reagents

1x PBS (Cellgro)

3-(4,5-Dimethylthiazol-2-yl)-2,5-diphenyltetrazolium bromide (Fischer scientific)

Acetic acid (VWR)

Acrzlamide/Bisacrylamide (Bio-Rad)

Agarose (Roth)

Agarose low melting point (Fischer Scientific)

Bovine Serum Albumine (Omega Scientific)

Carboxymethylcellulose (Sigma)

Crystal Violet (Sigma)

Diaminoethanetetraacetic acid (Fischer Scientific)

Dimethyl sulfoxide (Sigma)

DMEM medium (Gibco)

dNTP-Mix (Fermentas)

Ethanol (VWR)

Fetal Bovine Serum (Mediatech)

Formaldehyde (Carl Roth)

Freezing Medium (synth-a –Freeze, Fischer)

GelRed (Biotium)

Glycerol (Fisher Scientific)

Isoflurane (VetEquip)

Isopropanol (Carl Roth)

Methanol (Carl Roth)

Penicillin/Streptomycin solution (Gibco)

Protease inhibitors mix Complete Mini (Roche)

Protein Inhibitor cocktail (Roche)

Restriction enzymes (Neblabs)

RPMI medium 1640 (Gibco)

Sodium azide (Sigma)

Sodium dodecyl sulfate (Fisher Scientific)

Stemulate Medium (Cook Medical)

Taq DNA polymerase (Fermentas)

Tris-Base (Fisher Scientific)

Tris-HCL (Fisher Scientific)

Triton X-100 (Sigma)

Trypan Blue (Cellgro)

Trypsin-EDTA (Gibco)

Tween 20 (Bio-Rad)

3.1.3. Kits

Absolute™ QPCR SYBR Green Mix (Thermo Fisher)

DNA-free (Ambion)

Mouse IFNg ELISA Ready-SET-Go (eBioscience)

Mouse IL-2 ELISA Ready-SET-Go (eBioscience)

Phusion DNA Polymerase F-530L (Finnzyme)

PowerUp™ SYBR™ Green Master Mix (Thermo Fisher)

QIAquick PCR Purification kit (Roche)

RevertAid First Strand cDNA Synthesis Kit (Thermo Scientific)

Transcriptor High Fidelity cDNA Synthesis Kit (Roche)

Velocity DNA Polymerase (Bioline)

Xfect (Clontech)

Zymoclean™ Gel DNA Recovery Kit (Zymo Research)

3.1.4. Buffers and solutions

DMEM 10%

10% FBS

1% pen/str

DMEM

DMEM 2%

2% FBS

1% pen/str

DMEM

Overlay Medium

CMC 15g

DMEM 1000 ml

Pen/Strep 1%

FBS 5%

Crystal Violet Staining Solution

Crystal Violet 1.3g

Methanol 50 ml

37% Formaldehyde 300 ml

Water 650 ml

Tissue Lysis Buffer pH 7.6

TAE Buffer (50x)

Tris-Base 242 g

0.5M EDTA pH 8.0 100ml

Acetic acid 57.1 ml

TBE Buffer (10x) pH 8.3

Tris Base 108g

Boric acid 55g

0.5M EDTA pH 8.0 40ml

TB Medium

47 g Terrific Broth

4 mL glycerol

dH2O to 1 L

TB plate (15 ml of TB agar per 10 cm plate)

23.5 g Terrific Broth

7.5g Agar

2 mL glycerol

dH2O to 500mL

3.1.5. Antibodies

CD105	Invitrogen
CD14	BD biosciences
CD146	BD biosciences

CD31	BD biosciences
CD34	BD biosciences
CD44	BD biosciences
CD45	BD biosciences
CD90	BD biosciences

3.1.6. Bacteria and cell lines

Dh5α	competent E. coli bacteria strain
A549	human lung adenocarcinoma cell line
B16F10	murine melanoma cell line
4T1	murine mammary carcinoma cell line
CV-1	African green monkey kidney fibroblast cell line
HEK 293T	Human kidney fibroblasts

hADSCs chosen for the study were obtained by culturing SVF of various healthy donors and kindly provided by StemImmune inc.

3.1.7. Oligonucleotides

Name	Sequence (5’ – 3’)
FLUCF3	CCAGGGATTTCAGTCGATGT
FLUCR3	AATCTGACGCAGGCAGTTCT
mGAPDHF1	AACTTTGGCATTGTGGAAGG
mGAPDHR1	ACACATTGGGGGTAGGAACA
EGFPF1	ACGTAAACGGCCACAAGTTC
EGFPR1	AAGTCGTGCTGCTTCATGTG
A56RR	CATCATCTGGAATTGTCACTACTAAA
A56RF	ACGCCGACAATATAATTAATGC

3.1.8. Animal use

4-5 week old female BALB-c and C57BL/6 mice were purchased from Harlan Laboratories, Inc, USA. 5-6 weeks old female athymic nude mice, Hsd: Athymic Nude-Foxn1nu, were purchased from Charles River, Germany. BALB-c and C57BL/6 mice were cared for and maintained according to animal care regulations under Genelux approved protocol by the Institutional Animal Care and Use Committee of Explora Bio labs, Inc (San Diego, CA, USA). Athymic mice were cared for under an approved protocol by animal welfare regulations of the government of Upper Franconia, Germany, and conducted according to the German animal protection guidelines (permit number: 55.2.2.-416 2532-2-344)

3.1.9. Recombinant Vaccinia viruses

All recombinant Vaccinia viruses were provided by Genelux Corp, San Diego, USA, and/or StemVac Corp, San Diego, USA. GLV-1h68 was described earlier [91]. GLV-6b500 is a Copenhagen (clone 15.1.1) strain backbone recombinant Vaccinia virus with an insertion of the far-red fluorescent protein TurboFP635 expression cassette into J2R gene of the virus genome under control of synthetic early-late promoter (pSEL), GLV-6b540, GLV-6b541, GLV-6b542 are Copenhagen strain backbone viruses with murine IL-2 gene expression cassette insertion into J2R gene under the control of early (pSE), pSEL or late (pSL) promoters, respectively. GLV-6b528, GLV-6b529, GLV-6b530 are Copenhagen strain backbone viruses with murine IFNg gene expression cassette insertion into J2R gene under the control of pSE, pSEL, or pSL promoters, respectively. GLV-2b372 is a LIVP1.1.1 backbone virus strain with turboFP635 gene expression cassette in naturally disrupted J2R locus of the virus genome, described earlier [92]. GLV-2b537, GLV-2b538, GLV-2b539 are LIVP1.1.1 backbone viruses with murine IL-2 gene expression cassette insertion into J2R gene under the control of pSE, pSEL, or pSL promoters, respectively. GLV-2b525, GLV-2b526, GLV-2b527 are LIVP1.1.1 backbone viruses with murine IFNg expression cassette insertion into J2R gene under the control of pSE, pSEL, or pSL promoters, respectively. LIVP1.1.1, COP15.1.1, and ACAM2000 virus strain served as a control. Schematic representations of recombinant Vaccinia virus strains used in the study are presented in **Fig. 1**.

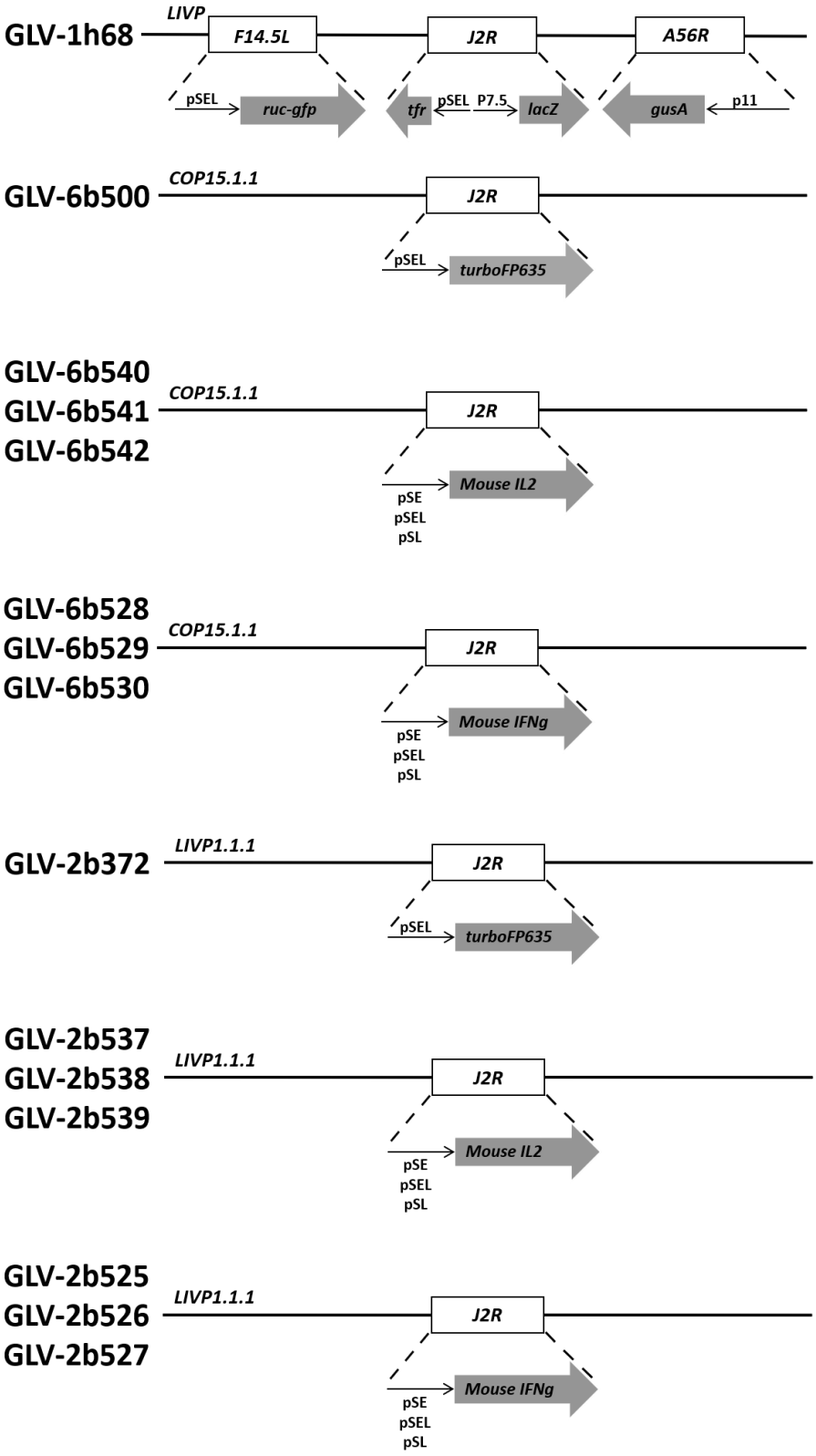

Fig. 1. Schematic representations of recombinant Vaccinia virus strains used in the study.

3.2. Methods

3.2.1. Cell culture and passaging

All the cell cultures used in the study have been carried out under sterile conditions and were grown in a humidified 5% CO2 incubator at 37°C. Depending on a cell line, the cells were cultured in cell culture dishes, flasks, or well plates of different sizes and cell culture mediums of different compositions. The medium was regularly changed to ensure the cells are not cultured in an exhausted medium. Cells were passaged upon reaching 80-90% confluence. For that, cells were washed twice with PBS and incubated with EDTA-Trypsin or TrypLE until they become detached from the cell culture vessel surface (usually, 2 to 5 minutes, depending on a cell line). The cells were then washed off the surface with a cell culture growth medium (MG^{2+} and CA^{2+}), resuspended, and counted using a TC20 automated cell counter. At this point, the cells are ready to be passaged at the desired ratio.

3.2.2. Freezing and thawing of cells

Cells in suspension were centrifuged for 5 min at 300g at room temperature (r.t.), cells then resuspended in freezing medium, aliquoted into cryotubes, and put into freezing boxes, designed to be cooled by 1°C/min when at -80°C. The next day, cryotubes were transferred into a liquid nitrogen tank, where they can be preserved for long-term storage.

For thawing, cryotubes with frozen cells were placed into a water bath at 37°C until the suspension is mostly defrosted. The cells were then resuspended in 10 ml of fresh cell culture medium, centrifuged for 5 min at 300g at r.t., resuspended again, and incubated in a cell culture vessel a 37°C incubator with 5% CO2.

3.2.3. Isolation of hADSCs

hADSC were isolated from a human stromal vascular fraction (SVF) provided by non-cancerous donor patients with consent at clinics in Rancho Mirage and Berkeley Hills, CA, USA. At passages, 2-3 isolated hADSCs were transferred to the University of Wuerzburg for characterization and further research. The cells then were characterized by their fibroblast morphology when adherent; by their ability to differentiate into cells with adipogenic, chondrogenic, or osteogenic phenotypes. The cells were also immunophenotyped with flow cytometry by using CD14, CD31, CD34, CD44, CD45, CD90, CD105, and CD146 antibodies.

3.2.4. Virus titer determination assay

To determine virus replication capacity in cells of different origins, the cells were infected with the virus at different multiplicities of infection (MOI) in a low volume of cell culture medium containing 2% FBS for 1 hour at 37°C in 5% CO2, with the gentle swirling of the cell culture vessel every 15 min. The medium was then exchanged with a fresh cell culture medium containing 5% FBS. Infected cells were harvested with either EDTA-Trypsin or cell scraper at 3, 24, 48, 72, and 96 hours post-infection (hpi) and were frozen at -80°C together with supernatant. After three freeze-thaw cycles, the samples were sonicated three times at maximum sonication level for 30 sec each time.

To prepare samples from mouse tissues, the organs of interest were homogenized in PBS (double the volume of tissue) in Whirl-Pac Homogenizer Blender bags. After three freeze-thaw cycles, the samples were sonicated three times at maximum sonication level for 1 min each time.

To determine the number of effective virus particles in the samples, a standard plaque-forming assay on CV-1 cells was performed. For that, the sonicated samples were serially diluted in a

DMEM cell culture medium containing 2%FBS and 0.2 ml of each dilution put onto 24-well plates with 100% confluent CV-1 cell monolayers in duplicates. After 1h incubation at 37°C in 5% CO2 with gentle swirling every 15 min, 1 ml of overlay medium was added to each well. After two days of incubation at 37°C in 5% CO2, the cell monolayers were stained with crystal violet solution. Plaques were counted on LightPad and virus titer in PFU/ml was determined according to the dilution.

3.2.5. Cell viability determination assay

The viability of the cell was determined by assessing the ability of their mitochondria to convert 3-(4,5-Dimethylthiazol-2-yl)-2,5-diphenyltetrazolium bromide (MTT) into formazan crystals [93]. The cells are plated in 96-well plates and infected in triplicates with the virus at different MOIs upon reaching 80-90% confluence. At 24, 48, 72, and 96 hpi, MTT solution was added to the cells at a final concentration of 0.5 mg/ml. The cells were then incubated until formazan crystals are formed (2-3 hours, depending on the cell line). The crystals were dissolved with either DMSO or 10% HCl in isopropanol and absorbance was measured at 570 nm wavelength with 620 nm reference. The viability of uninfected cells was considered to be 100% and served as a control.

3.2.6. Tumor implantation and monitoring

$1x10^5$ 4T1 breast cancer cells were implanted into the fat pad of 5-6 weeks old female BALB/c mice (5 mice/group) to establish a syngeneic orthotopic murine tumor model.

$2x10^5$ B16F10 melanoma cells were subcutaneously implanted into the right flank of 5-6 weeks old female C57Bl/6 mice (5 mice/group) to establish a murine melanoma model.

$5x10^5$ A549 human lung adenocarcinoma cells were subcutaneously implanted into the right flank of 5-6 weeks old female Athymic Nude-Foxn1nu mice.

The mice were monitored for swelling of the foot pad or the flank and any other adverse reactions to the implantation. The growth of the tumors was measured daily once the tumors become palpable. Tumors were measured using a digital caliper and the tumor volume was calculated as length, multiplied by width, multiplied by 0.52.

3.2.7. Tumor therapy

Once tumors reached 200 mm^3 (450 mm^3 for A549 xenograft model), they were treated with the virus, combination therapy with romidepsin or cyclophosphamide (CPA), or hADSCs loaded with the virus, depending on the tumor model. The virus was injected retro-orbitally, intravenously through the tail vein, or intratumorally. Romidepsin and CPA were given intraperitoneally, 0.25 ug/kg of romidepsin, and 35, 100, or 210 mg/kg of CPA, depending on the design of the experiment.

hADSCs were infected at either 4 or 100 MOI for 1 hour at 37°C in DMEM cell culture medium with no FBS added and injected either intravenously through the tail vein or intratumorally.

3.2.8. Real-time quantitative polymerase chain reaction (RT qPCR)

To detect viral DNA in tissues of treated animals, the animals were dissected and the organs of interest (brain, heart, lungs, spleen, kidneys, liver) and tumors were homogenized in PBS with protease inhibitors with Fast-Prep-24 homogenizer 4 times for 30 sec each. DNA was isolated by using the DNeasy Blood and Tissue kit according to the kit protocol. DNA concentration was determined by an absorbance reader at 260 nm. 400 ng of total DNA was used for PCR reaction,

which was carried out in PowerUp Cyber green mix solution. The reaction was run using the following protocol: 5 minutes for initial enzyme activation at 95°C, and then 59 cycles of 30-sec denaturation at 95°C, 30-sec annealing at 55-65°C gradient (due to different primer annealing temperature), 30-sec extension at 72°C and imaging. To check product specificity, melting curves were built from 55°C to 90°C and the products were analyzed by gel electrophoresis to ensure that they have the right size. GAPDH was used for normalization as a reference gene.

3.2.9. Gel electrophoresis

0.6g of low melting point agarose dissolved by heating in 33 ml of 1x TBE buffer were cooled down to 40-50°C. 3.3 ml of 10000x GelRed were added to the solution. The solution was poured into a gel chamber with a 15-pocket insert. After solidification, the gel was put into a gel electrophoresis chamber of Mini-Sub Gell GT filled with 1x TBE buffer with GelRed, insert was removed and pockets were filled with RT qPCR products mixed with loading dye. GeneRuler DNA ladder was used as a reference. The gel was run at 90V using PowerPac Basic for 40 min. The gel was scanned by Transilluminator and the size of the products was assessed using the DNA ladder as a reference.

3.2.10. Enzyme-linked immunosorbent assay (ELISA)

A “sandwich” ELISA (based on the binding of two monoclonal antibodies) was used to detect the presence of IFNg and IL-2 in the blood of treated animals. For detecting murine IFNg and IL-2 respective ELISA kits were used. The plates were coated with capture antibodies according to the manufacturer’s protocol. Standards and samples were added to the wells at 1:50 and 1:100 dilution and incubated at r.t. for 2 hours. Detection antibodies were added and incubated as noted by the manufacturer. After washing, the plates were incubated with horseradish(HRP)-conjugated

streptavidin. Unbound to biotinylated detection antibodies streptavidin was washed away and tetramethylbenzidine (TMB) was added as substrate. The reaction was stopped by 0.5N sulphuric acid. Color intensity (which corresponds to the amount of IFN or IL-2 in the sample) was measured by spectrophotometer at 450 nm wavelength with 570 nm reference. All the samples and standards were done in duplicates. Blood serum was obtained by retro-orbital blood sampling followed by serum separation after the blood was allowed to clot.

3.2.11. Lentivirus production and generation of lentiviral transgenic cells

pLV-EF1A-EGFPKir7.1 (**Fig. 2**) and pLenti PGK Blast V5-LUC (**Fig. 3**) plasmid-containing Dh5α bacteria were streaked on ampicillin TB agar plates. The next day, single colonies were put in 5 ml of TB starter culture with ampicillin and incubated for 6-8 hours at 37^{0}C. After that 10 µl of starter culture were transferred to 10 ml of TB media with ampicillin and incubated overnight. The plasmids were then extracted according to the QIAGEN miniprep kit protocol. Final plasmid stock concentrations were assessed with a spectrophotometer. Diagnostic digests were performed to ensure the plasmids are of the expected size.

To generate lentiviral constructs, 293FT cells were seeded in 10 cm^{2} well plates 24 hours prior to transfection. 293FT cells were transfected with the amplified plasmids and packaging plasmids pMD2.G (Addgene #12259), psPAX2 (Addgene #12260) in presence of lipofectamine. The transfection medium was changed the next day and lentivirus was harvested and frozen down 2 days later.

A549 cells were transduced with pLenti PGK Blast V5-LUC lentivirus. Human adipose-derived stem cells from donor BH21 were transduced with pLV-EF1A-EGFPKir7.1 lentivirus and were grown in a cell culture medium containing 10 µg/ml of blasticidin for 14 days.

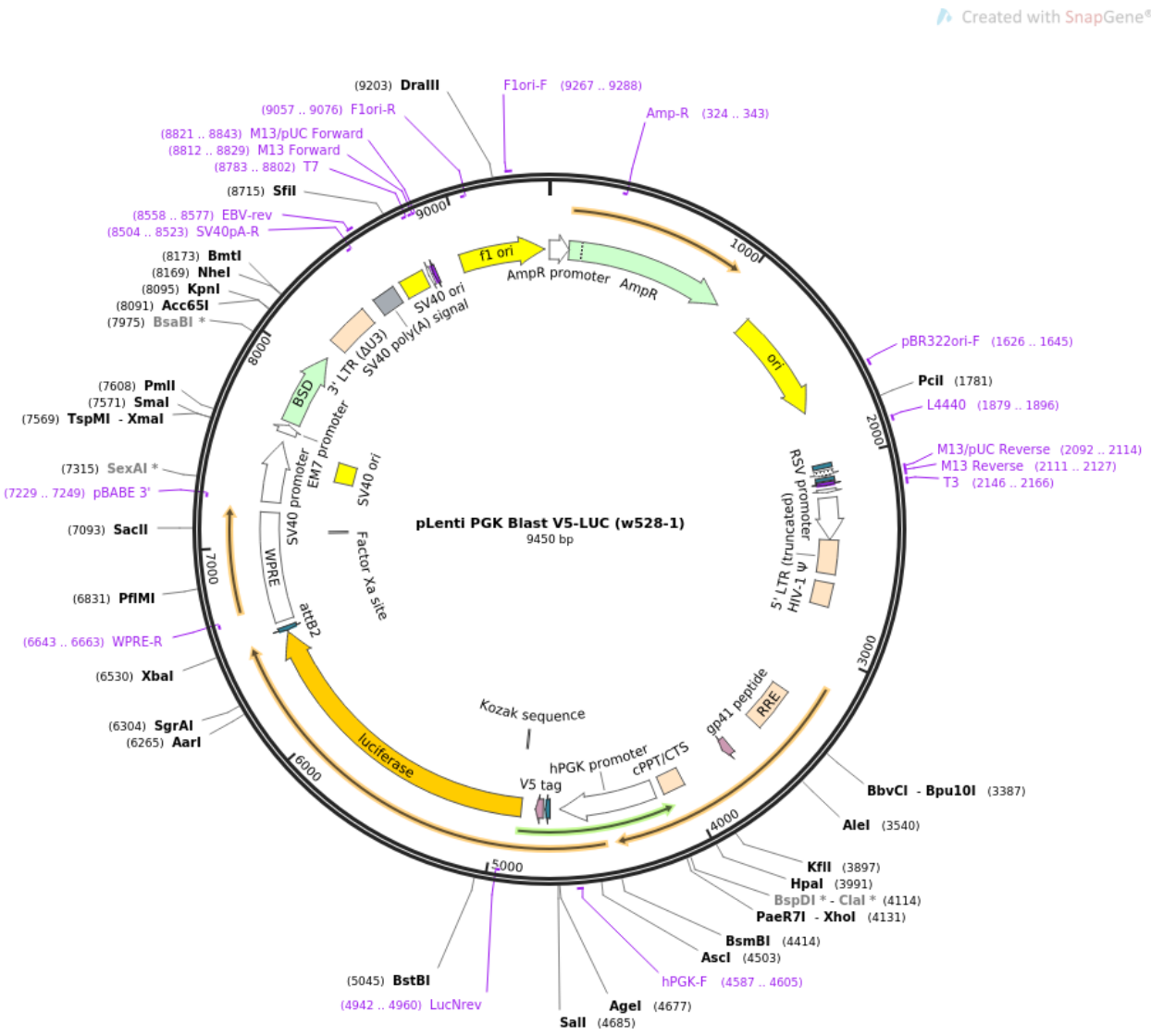

Fig. 2. Schematic diagram of pLV-EF1A-EGFPKir7.1 (Addgene #107181) plasmid

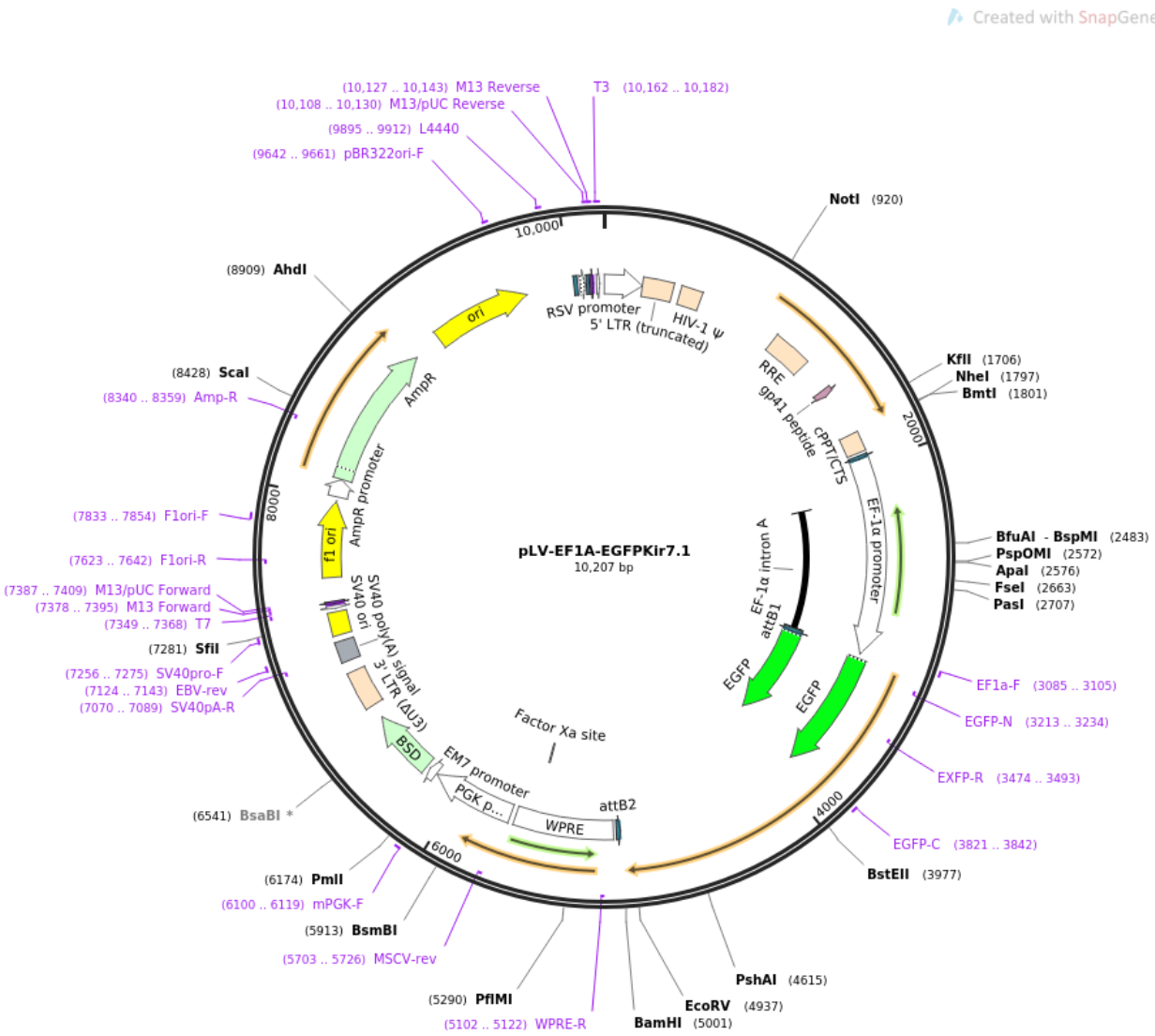

Fig. 3. Schematic diagram of pLenti PGK Blast V5-LUC (addgene #19166) plasmid

3.2.12. Viability determination by flow cytometry

The cells of interest were stained by Viability Dye eFluor™ 520 according to the manufacturer's protocol and analyzed on the Accuri C6 flow cytometer. Heat-killed cells (65°C for 1 min) served as a positive control.

3.2.13. Statistical analysis

Two-tail Student's t-test was used for the analysis of statistically significant differences between treatment groups. Differences in survival rates were analyzed with the log-rank test. P values of <0.05 were considered statistically significant.

CHAPTER 4: RESULTS

4.1. IL-2 and IFNg expressing Vaccinia viruses in various immunocompetent mouse models

4.1.1. Virus production analysis in infected 4T1 cells

To analyze the impact of gene modifications on the ability of the viruses to replicate in tumor cells of interest, 4T1 murine breast carcinoma cells (passage 28) were infected with corresponding viruses and harvested after 3, 24, 48, 72, and 96 hours after infection as described in paragraphs 3.2 and 3.3. Standard plaque assay was conducted following paragraph 3.2.4 of the "Methods" section. Replication of viruses based on the LIVP1.1.1 clone was directly compared to replication of GLV-2b372 virus, and replication of COP1.1.1-based viruses was compared to GLV-6b500. According to the data presented on the virus replication curves, all the COP1.1.1-based viruses possess significantly stronger (on average a 100-fold difference) replication ability in 4T1 murine breast carcinoma cells when compared to LIVP1.1.1 backbone viruses (**Fig. 4**). When it comes to the payload burden, IL-2 has no to almost no impact on virus amplification in the cells when compared to TurboFP635, while IFNg significantly impairs virus replication, especially in the case of COP1.1.1 backbone viruses.

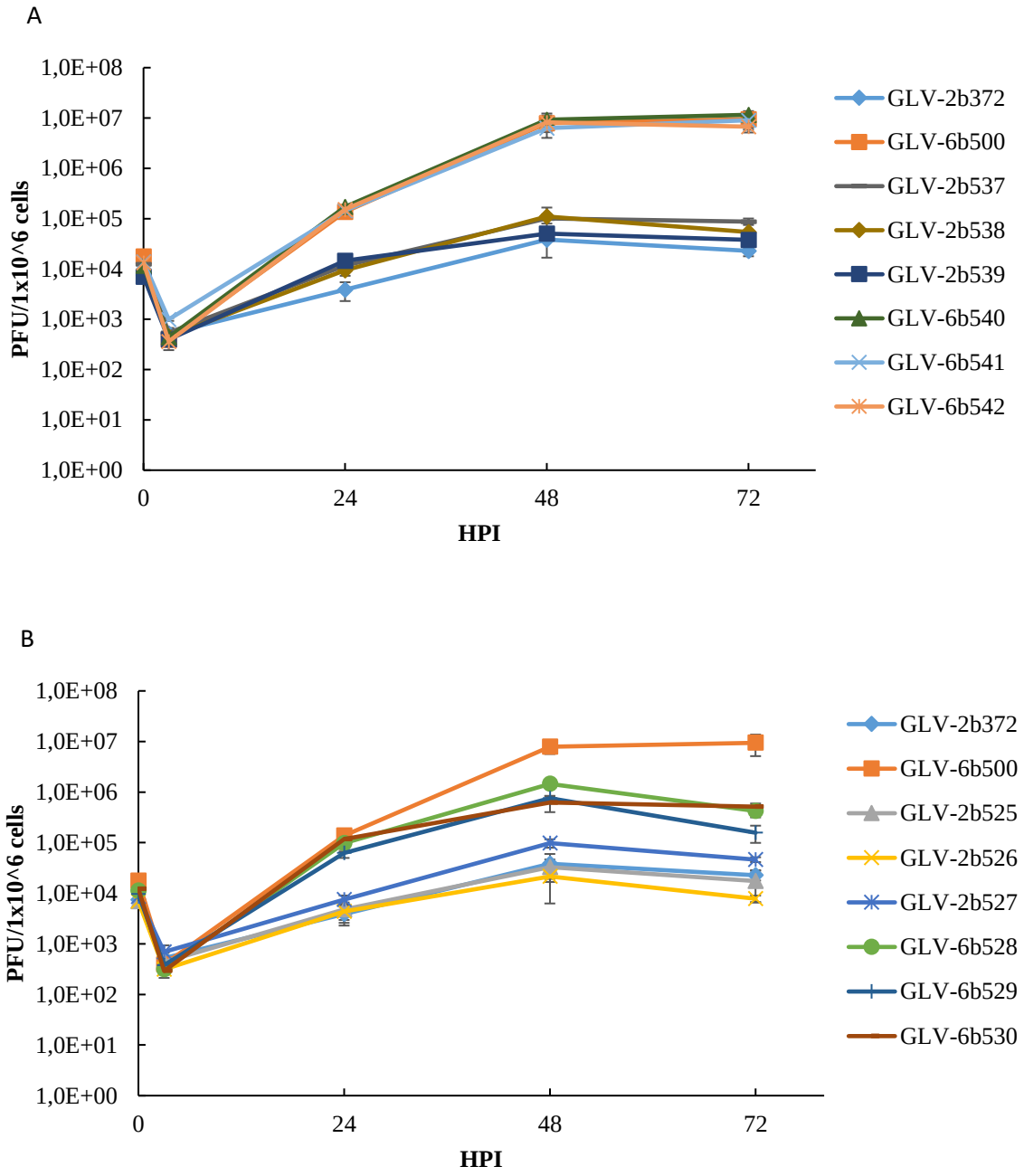

Fig. 4. Vaccinia virus replication in 4T1 breast carcinoma cells. **A.** Replication of LIVP and COP backbone Vaccinia virus strains carrying murine IL-2 expression cassette in comparison to GLV-2b372 and GLV-6b500. **B.** Replication of LIVP and COP backbone Vaccinia virus strains carrying murine IFNg expression cassette in comparison to GLV-2b372 and GLV-6b500. The values are the mean of the triplicates, bars indicate ±SD.

4.1.2. Effect of a single dose of IL-2 and IFNg expressing Vaccinia virus in 4T1 bearing BALB/c mice

To access the oncolytic properties of the investigated viruses, a syngeneic animal study was designed. $1x10^5$ 4T1 breast carcinoma cells were implanted into orthotopic fat pads of 5-6 week old female BALB/c mice. $5x10^7$ pfu/animal were administered retro-orbitally in 100 ul of PBS once average tumor volume reached 200 mm^3. Mice were sacrificed after either tumor size exceeded 4500 mm^3 or observed net body weight loss reached 15% or more.

4.1.2.1 Tumor growth and survival

According to the results of the animal study, all of the Copenhagen backbone viruses neither slowed down tumor growth nor affected the survival of the animals. Treatment with two of the LIVP backbone viruses, GLV-2b537 (IL-2 under control of the early promoter) and GLV-2b538 (IL-2 under control of the early-late promoter) resulted in significantly increased survival of the animals as well as in delay in 4T1 tumor growth. For clarity, non-pSEL promoter virus constructs are excluded from tumor growth and Kaplan-Meier survival curves (**Fig. 5**). Instead, they are included in the overall panel of therapeutic efficacy and survival benefit of all the tested strains (**Fig. 6**).

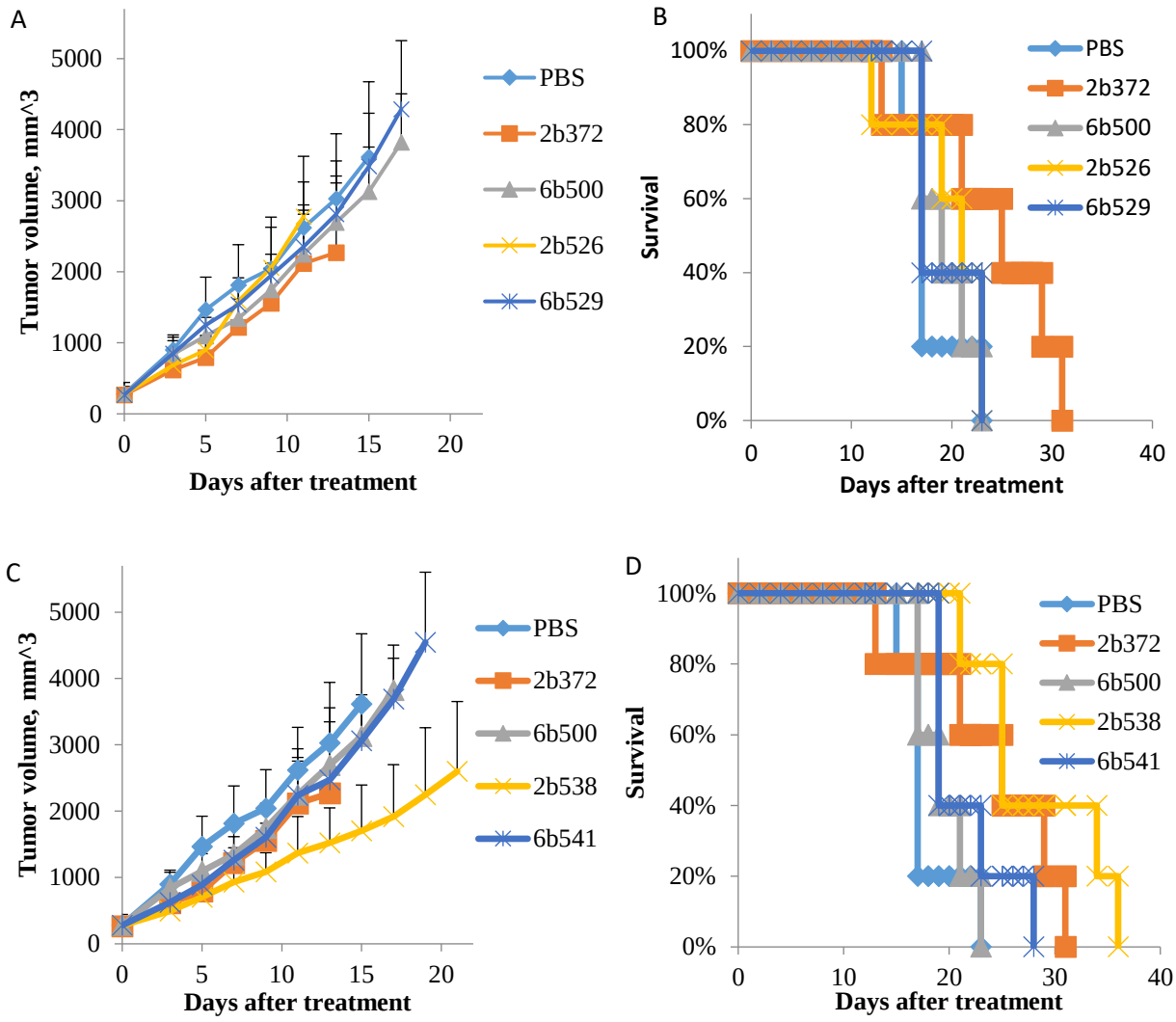

Fig. 5. Vaccinia virus in orthotopic 4T1 breast carcinoma BALB/c mouse model. **A.** Curves of tumor growth in 4T1 tumor-bearing BALB/c mice treated with LIVP and COP backbone Vaccinia virus strains carrying IFNg under control of pSEL promoter (GLV-2b525 and GLV-6b528, respectively). **B.** Kaplan-Meier survival curve in groups treated with LIVP and COP backbone Vaccinia virus strains carrying IFNg under control of pSEL promoter (GLV-2b525 and GLV-6b528, respectively). **C.** Curves of tumor growth in 4T1 tumor-bearing BALB/c mice treated with LIVP and COP backbone Vaccinia virus strains carrying IL-2 under control of pSEL promoter (GLV-2b538 and GLV-6b541, respectively). **D.** Kaplan-Meier survival curve in groups treated

with LIVP and COP backbone Vaccinia virus strains carrying IL-2 under control of pSEL promoter (GLV-2b538 and GLV-6b541, respectively). * - a statistically significant difference. Bars indicate standard deviation.

Virus strain	Therapeutic efficacy	Survival benefit
GLV-6b500	-	-
GLV-6b528	-	-
GLV-6b529	-	-
GLV-6b530	-	-
GLV-6b540	-	-
GLV-6b541	-	-
GLV-6b542	-	-

Virus strain	Therapeutic efficacy	Survival benefit
GLV-2b372	+*	-
GLV-2b525	+	-
GLV-2b526	-	-
GLV-2b527	-	-
GLV-2b537	++	yes (p<0,05)
GLV-2b538	+++	yes (p<0,01)
GLV-2b539	+	-

Fig. 6. A. Overall chart of therapeutic efficacy and survival benefit in groups treated with COP backbone Vaccinia virus strains carrying IFNg or IL-2. **B.** Overall chart of therapeutic efficacy and survival benefit in groups treated with LIVP backbone Vaccinia virus strains carrying IFNg or IL-2. "+" – statistically significant difference in one or two time points, "++" – statistically significant difference in 3 or more time points., "+++" – statistically significant difference in all the time points.

4.1.2.2. Treatment toxicity based on body weight of the animals

Body weights of treated animals were accessed in order to analyze the virus- or payload-mediated toxicity of the treatment. Treatment with GLV-2b537 (LIVP with IL-2 under control of the early promoter) and GLV-2b538 (LIVP with IL-2 under control of the early-late promoter) resulted in immediate significant weight loss of the animals by day 3 after virus administration, with subsequent weight gain to day 7 (**Fig. 7**).

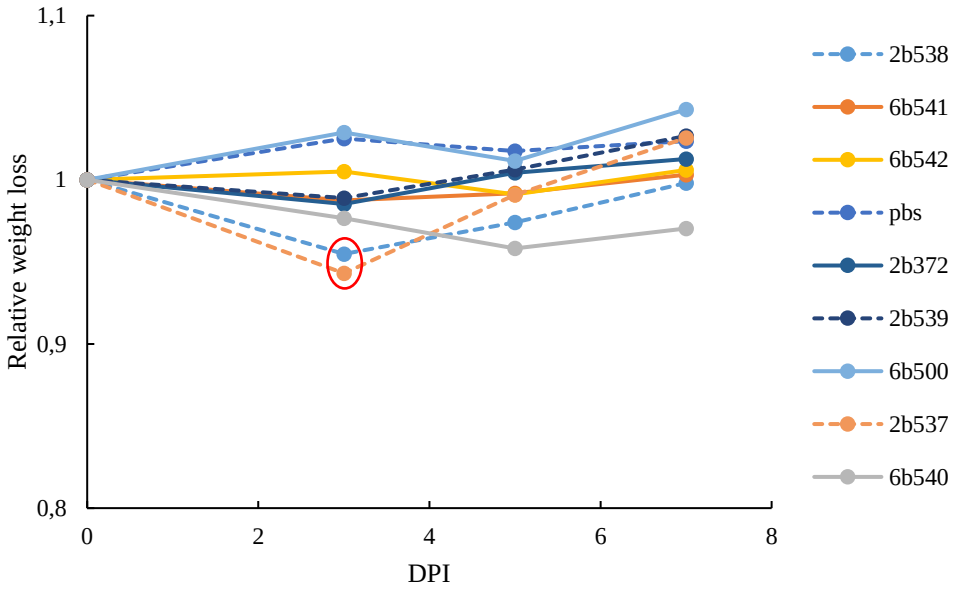

Fig. 7. Relative post-treatment weight loss in 4T1 bearing BALB/c mice treated with LIVP and COP backbone Vaccinia virus strains carrying IL-2; the weight of the animal equals 1 on the day of virus treatment. Weight loss in GLV-2b537 and GLV-2b538 groups on day 3 is marked with a red oval.

4.1.2.3. IL-2 and IFNg concentrations in blood of treated mice

IL-2 serum levels of treated animals were measured with ELISA on day 3 after virus injection. The only group where serum levels of IL-2 were above the detection limit was GLV-2b538 treated group (**Fig. 8**). The average IL-2 blood concentration in these mice was about 120 pg/ml. No IFNg was detected in the blood serum of animals after injection with IFNg-expressing viruses.

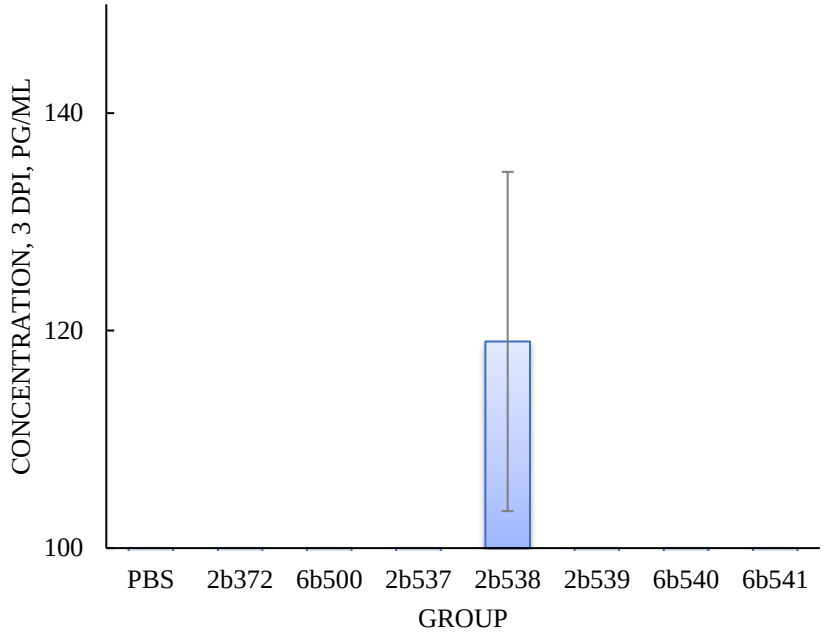

Fig. 8. IL-2 blood concentrations in 4T1 bearing BALB/c mice treated with LIVP and COP backbone Vaccinia virus strains carrying IL-2 on day 3 after injection. The bar indicates standard deviation.

4.1.3. Combination of IL-2 expressing Vaccinia virus with either cyclophosphamide or romidepsin in B16-F10 bearing C57BL6 mice

The next animal experiment was designed to study a combination of LIVP1.1.1 IL-2 expressing virus with chemotherapy. Two chemotherapeutic agents were chosen for the study, cyclophosphamide (CPA) and romidepsin. They were combined with the virus treatment independently from each other. $2x10^5$ B16F10 melanoma cells were implanted subcutaneously into the right flank of 5-6 week old female C57Bl/6 mice. Day 12 after the implantation, the animals were intraperitoneally injected with either 100 ug/kg of CPA or 0.25 ug/kg of romidepsin. $5x10^7$

PFU of the virus (either GLV-2b538 or GLV-2b372) was administered retro-orbitally two days after. Mice were sacrificed after either tumor size exceeded 4500 mm^3 or observed net body weight loss reached 15% or more.

4.1.3.1. Virus production in B16-F10 cells

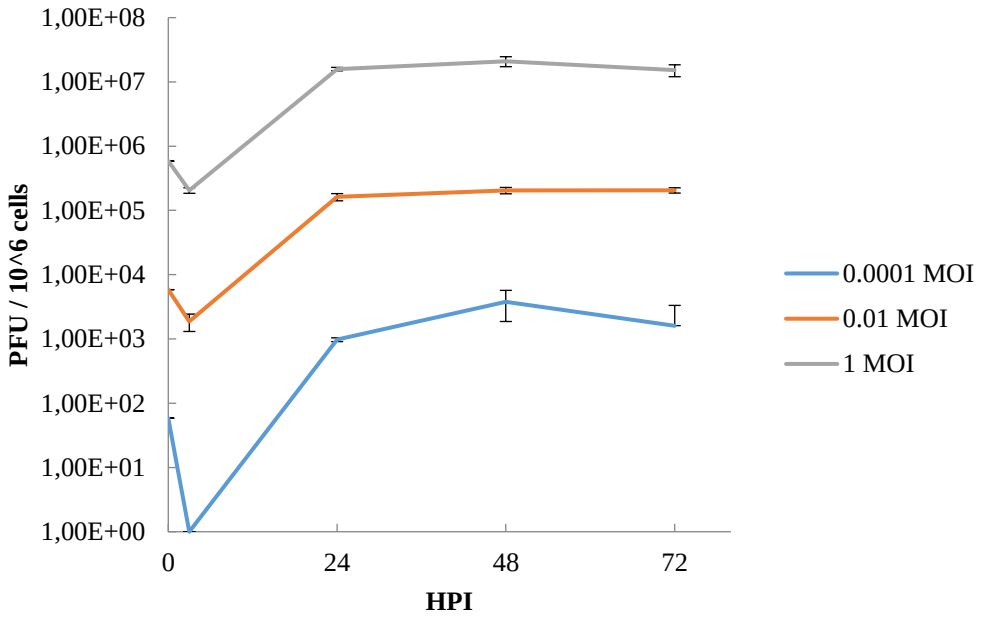

Fig. 9. GLV-2b538 replication in B16f10 murine melanoma cells. The values are the mean of the triplicates, bars indicate ±SD.

GLV-2b538 virus production was analyzed in B16F10 cells in culture. Melanoma cells were infected with the virus at different MOIs (0.0001, 0.01, and 1) and harvested at 3, 24, 48 and 72 hours after infection. Collected cells were prepared for the standard plaque assay on CV-1 cells. The assay was conducted according to the 3.2.4 paragraph. According to the results of three independent experiments, virus progeny was dependent on initial MOI and did not increase after 24 h after infection, meaning that new GLV-2b538 progeny produced by B16F10 cells wasn't able to infect these cells, but could successfully replicate in CV-1 cells (**Fig. 9**).

4.1.3.2. Tumor growth and survival

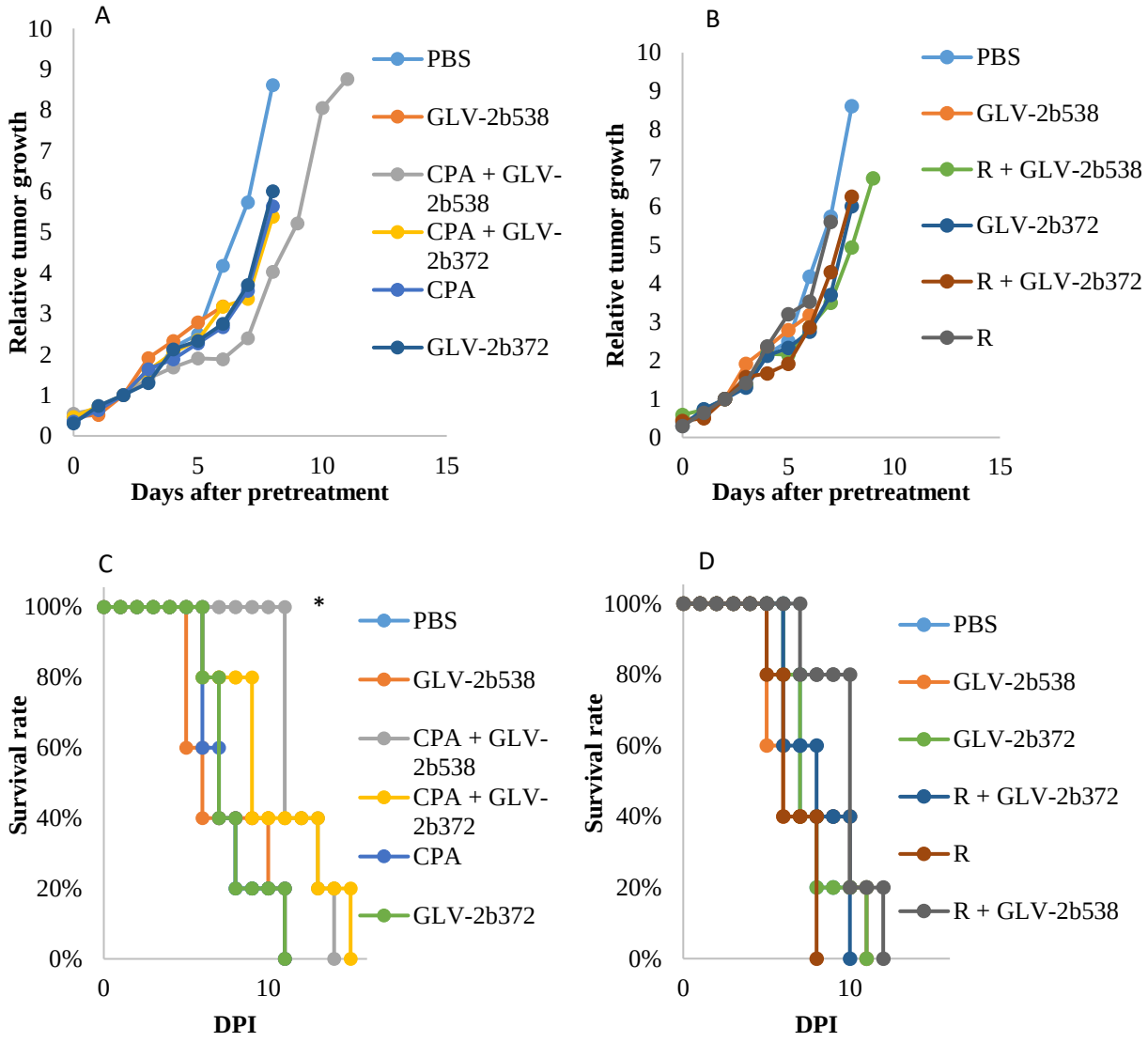

Fig. 10. Tumor growth and survival in B16 melanoma bearing mice treated with GLV-2b538 in combination with CPA or romidepsin. **A.** Tumor growth curves in CPA-pretreated groups. B. Tumor growth curves in romidepsin-pretreated groups. C. Kaplan-Meier curves in CPA-pretreated groups. **D.** Kaplan-Meier curves in romidepsin-pretreated groups. R – romidepsin, * - statistically significant difference.

The combination of the virus with romidepsin didn't result in a therapeutic benefit, except for slightly prolonged survival of mice treated with the combination in comparison with the animals that received only romidepsin intraperitoneally (**Fig. 10**). The combination of GLV-2b538 with CPA resulted in a slight delay of tumor growth (although not statistically significant) and significantly extended survival of mice from the combination group.

4.1.3.3. Analysis of treatment toxicity based on body weight of the animals

Treatment of B16 melanoma bearing C57Bl/6 mice with GLV-2b538 resulted in irreversible weight loss of the animals (**Fig. 11**). After a week after virus administration, most of the treated mice lost over 15% of their net body weight and had to be sacrificed. Mice treated with the combination of the virus and either CPA or romidepsin did lose a significant amount of weight but were able to gain it back within a week after the virus injection.

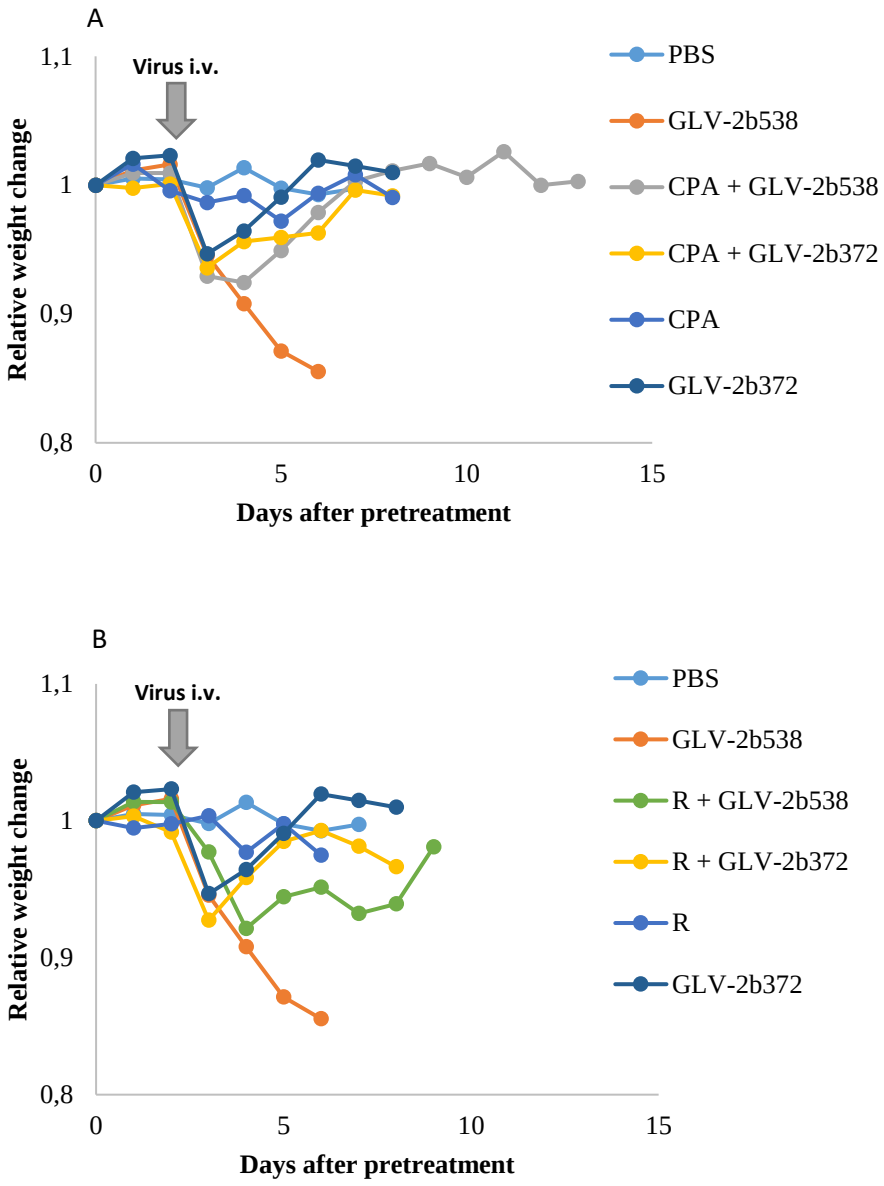

Fig. 11. A. Relative average weight change in mice treated with CPA, GLV-2b538 alone or in combination. **B.** Relative average weight change in mice treated with romidepsin, GLV-2b538 alone or in combination. R – romidepsin, CPA – cyclophosphamide

4.1.3.4. Virus titer determination in treated animals

The animals were dissected postmortem, and tumor, spleen, liver, kidneys, heart, lungs and brain were homogenized and virus titers were determined according to section 3.2.4.

mouse #	Spleen	Liver	Kidney	Heart	Lung	Brain	Tumor	day sacrificed/died	reason
38	0	0	0	0	0	0	7,60E+04	day 13	TuV
422	0	0	0	3,75E+03	2,11E+05	0	4,79E+08	day 8	FD
423	0	0	0	0	0	0	1,70E+02	day 12	TuV
424	2,31E+07	1,00E+04	0	6,14E+03	1,75E+04	3,00E+05	5,15E+07	day 7	FD
459	0	0	0	0	0	0	2,42E+07	day 7	weakness

Fig. 12. Endpoint virus titers (PFU/g) in B16 bearing C57BL/6 mice treated with GLV-2b538. TuV – the animal had to be sacrificed due to exceeding tumor volume; FD – the animal was found dead by animal handling personnel; weakness – the animal had to be sacrificed due to general weakness.

Virus distribution data in the animals from the GLV-2b538 group showed that the virus was preferentially colonizing the tumor site (**Fig. 12, Fig. 13**). In one week after injection, virus titers in the tumor site were about 10^7-10^8 PFU/g.

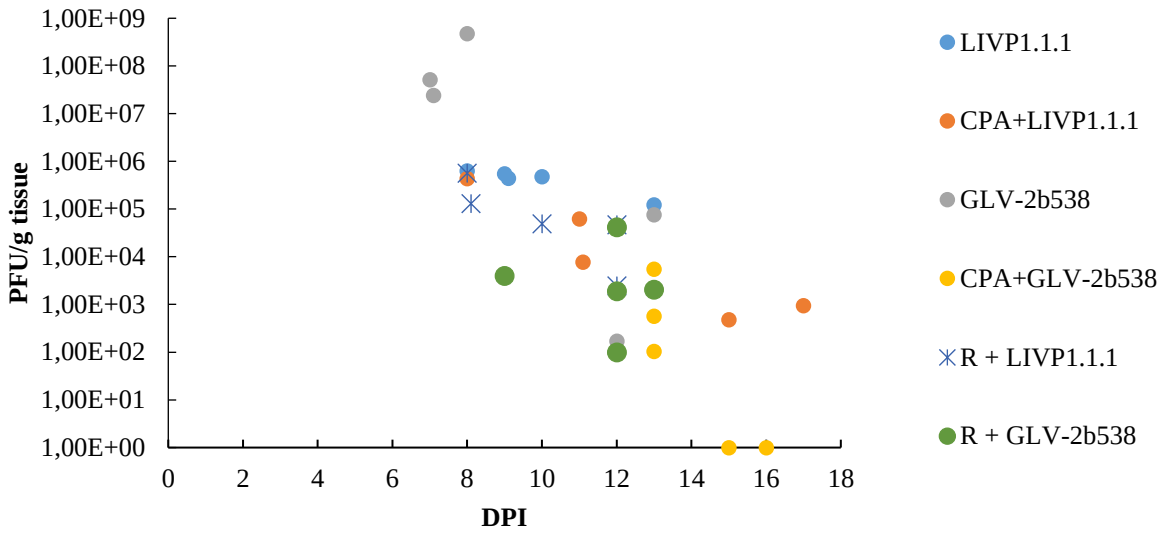

Fig. 13. Endpoint virus titers in tumors of treated animals. The data is represented in PFU per g of tissue.

Analysis of endpoint virus titers in the tumors of treated mice showed that the virus can still be found in the majority of the tumors at the point of elimination of the animal from the experiment due to weight loss/exceeding tumor volume/sickness. In this animal study, no specific groups were assigned to analyze virus distribution at a distinctive time point after treatment.

4.1.4. Dose-dependent effect of cyclophosphamide onto therapeutic efficacy of IL-2 expressing Vaccinia virus in B16-F10 bearing C57BL6 mice

To deeper study the combinatorial effect of CPA and GLV-2b538 during early stages of the treatment, another animal study was designed. Female 5-6 week old C57Bl/6 mice were subcutaneously injected with $5x10^5$ B16F10 cells/animal into the right flank. The virus ($5x10^7$ PFU/mouse) was administered retro-orbitally on day 7 after tumor cell implantation. Cyclophosphamide, either 210 mg/kg (high dose) or 35 mg/kg (low dose) was injected i.p. on either day 5, 7 or 9 after tumor cell implantation. Mice were euthanized on day 4 and day 7 after virus

injection in order to study virus colonization of the tumor and IL-2 and IFNg levels in tumor and blood of the animals.

4.1.4.1. Analysis of tumor growth

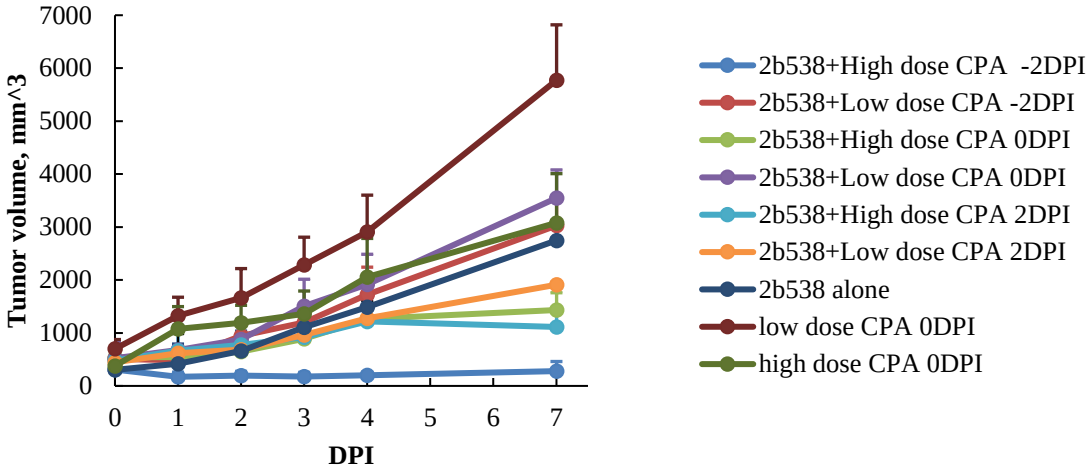

Fig. 14. Average tumor growth in mice treated with the combination of low/high dose of CPA and GLV-2b538. Bars indicate ±SD.

Although the experiment wasn't focused on the analysis of tumor growth and wasn't designed for it (due to the lack of a proper negative control group), we would still like to emphasize the effect of the combination on tumor development. All the combinations of CPA and the virus resulted in a significant delay in tumor growth when compared to low dose of CPA alone (**Fig. 14**). Treatment with the high dose of CPA two days before virus injection led to significant tumor shrinkage and a subsequent arrest of its growth until the end of the experiment.

4.1.4.2. Treatment toxicity based on body weight of the animals

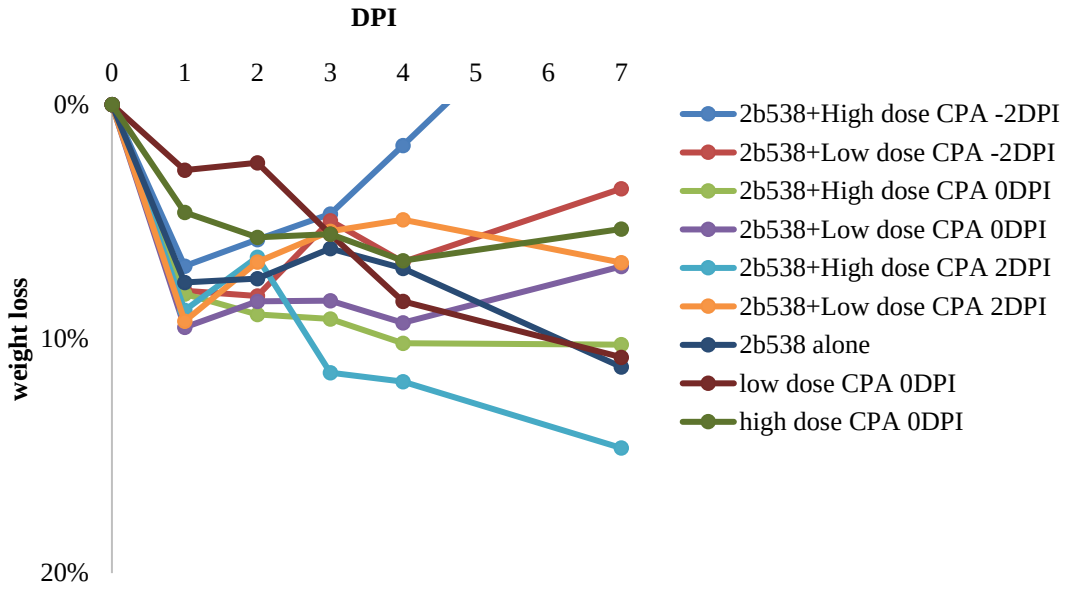

Fig. 15. Relative weight loss (in %) of mice treated with a combination of low or high dose of CPA in combination with GLV-2b538 at different time points.

Weights of the animals were measured daily to track possible treatment-mediated toxicity. The average net body weight in all experimental groups was falling starting day 1 after virus injection (**Fig. 15**). The only experimental animal group where the weight was quickly gained back was the group pretreated with the high dose of CPA.

4.1.4.3. Virus titers in B16-F10 melanoma tumor-bearing C57Bl/6 mice

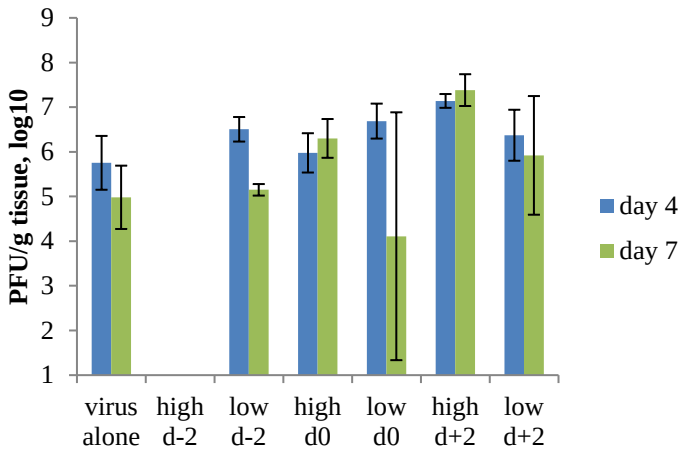

Fig. 16. Virus titers in tumors of mice treated with a combination of low or high dose of CPA in combination with GLV-2b538 at different time points. Bars indicate ±SD.

The virus was detected in all virus-treated experimental groups except for the one pretreated with the high dose of CPA (**Fig. 16**). On average, there was around 10^5 - 10^7 PFU/g of tumor detected both on day 4 and day 7 after virus administration.

4.1.4.4. IL-2 and IFNg in tumor and blood serum of treated animals

IL-2 and IFNg levels in tumor and blood were assessed with ELISA. The highest level of IL-2, both in serum and tumor was detected in mice treated with the high dose of CPA 2 days after virus injection (Fig. 17). In the group pretreated with the high dose of CPA, traceable levels of IL-2 could be found on both day 4 and day 7 in the blood serum, and on day 7 in the tumor site. In most of the groups, IL-2 levels in blood were strongly correlated with IL-2 levels in the tumor site. IFNg in the tumor site was detected in all virus-treated groups except for the one pretreated with the high dose of CPA.

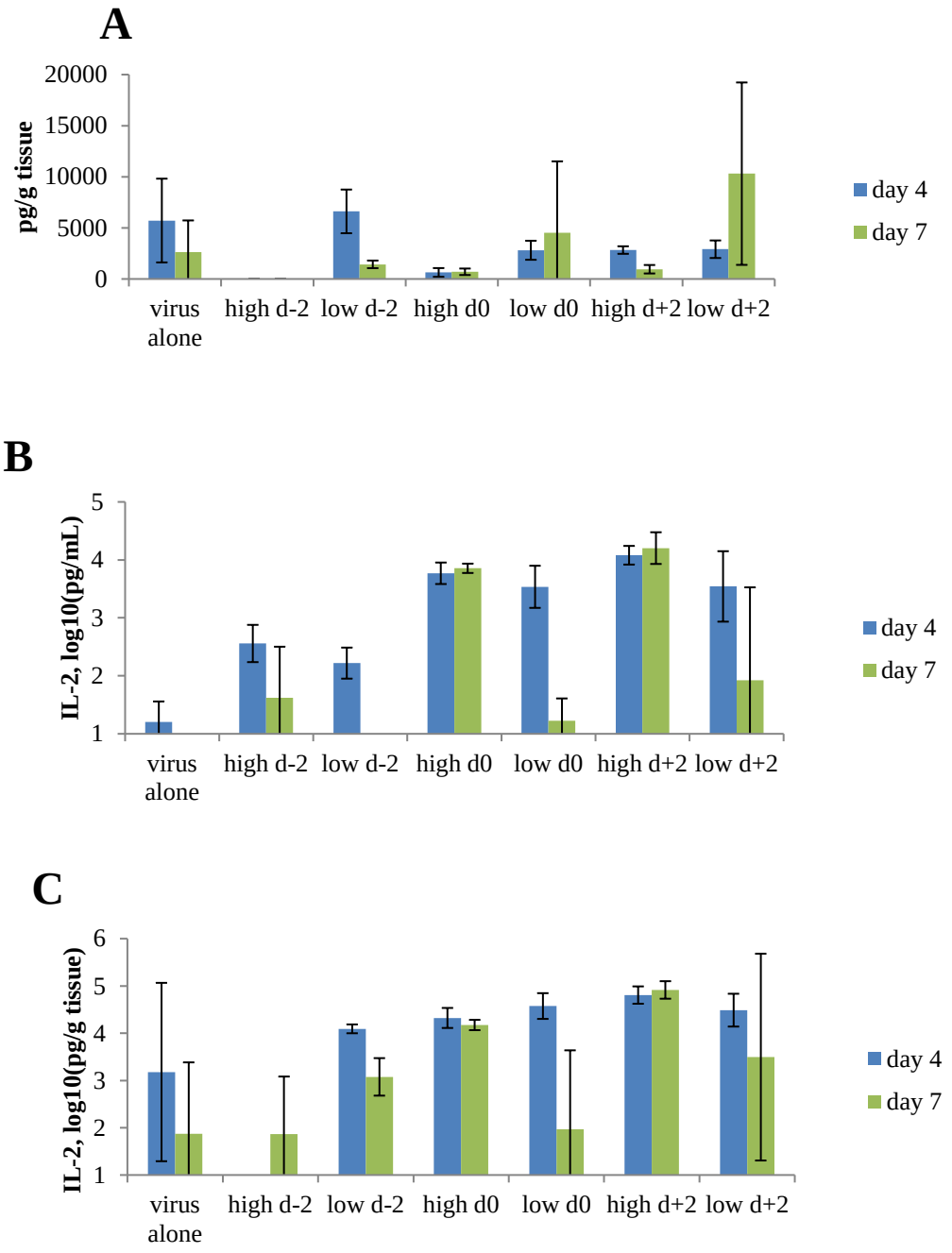

Fig. 17. IL-2 and IFNg levels in tumor and blood of animals treated with a combination of low or high dose of CPA in combination with GLV-2b538 at different time points. **A.** IFNg in the tumor at days 4 and 7. **B.** IL-2 in blood serum, day 4 and day 7. **C.** IL-2 in the tumor site, day 4 and day 7. Bars indicate ±SD.

4.2. Virus-loaded hADSCs as a Trojan horse therapy

4.2.1. Generation of GFP-expressing human adipose-derived stem cells

For tracking of hADSCs both *in vitro* and *in vivo*, we inserted eGFP under control of EF1alpha promoter into BHSD0021 hADSCs using 3rd generation lentiviral system as described in section 3.2.11 of the current work. The phenotype of the transfected cells was observed under a fluorescent microscope and expression of GFP was confirmed (**Fig. 18**).

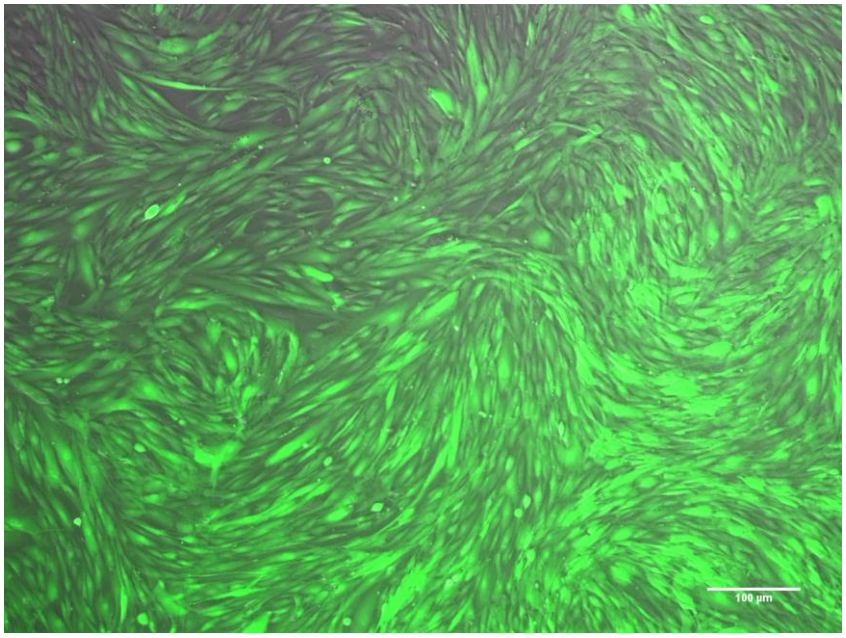

Fig. 18. BHSD0021-GFP hADSCs were derived from BHSD0021 cells by transfection with pLV-EF1A-EGFPKir7.1 lentivirus followed by blasticidin selection. The GFP expression is presented as a green signal. The scale bar is 100 µm.

4.2.2. Analysis of virus replication in human adipose-derived mesenchymal stem cells

GFP-expressing hADSCs were infected with 1 MOI of GLV-2b372 and expression of TurboFP635 was analyzed under a fluorescent microscope. The images indicate that the virus can productively replicate in hADSCs (**Fig. 19**).

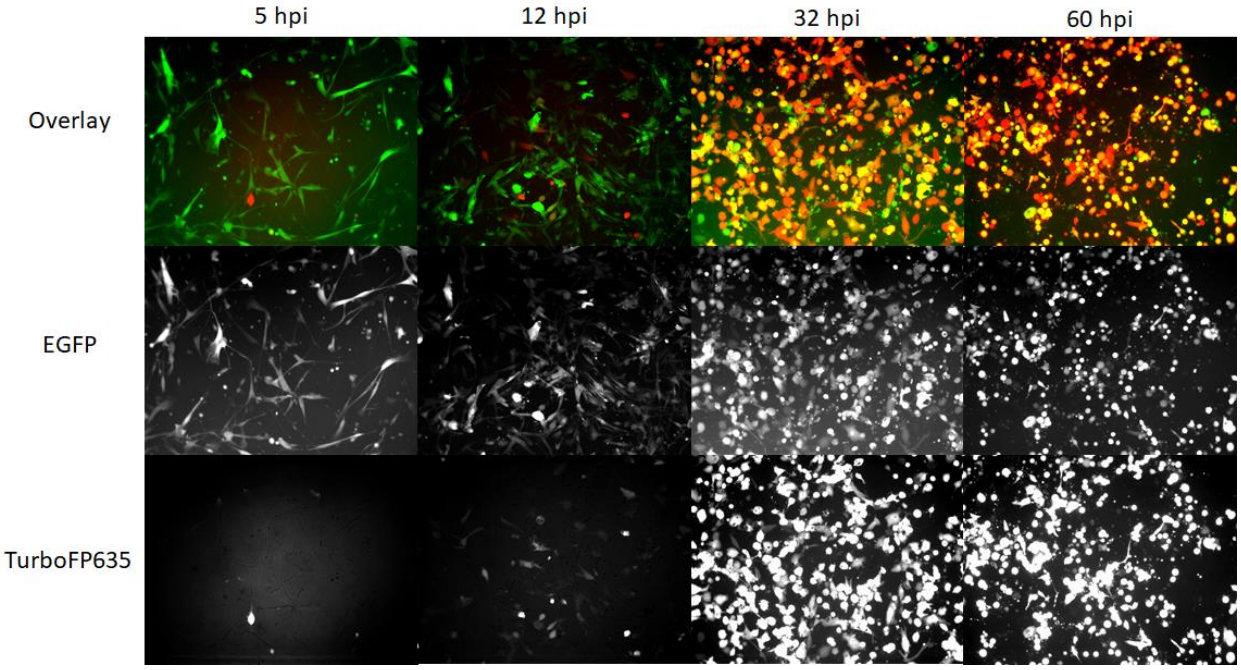

Fig. 19. GLV-2b372 replication in BHSD0021-GFP hADSCs. Virus-positive cells are expressing Turbo-FP635 (red).

To better understand the permissivity of hADSCs to Vaccinia virus, BHSD0021 and BHSD0022 hADSCs were infected with GL-1h68, GLV-2b372 or ACAM2000 at MOI of 0.01. All the strains tested replicated in both cell lines, but with different efficacy (**Fig. 20**). BHSD0021 was significantly more permissive to Vaccinia virus infection, having on average half-log to log difference in virus yield compared to virus yield in BHSD0022 cells under the same culturing conditions. GL-1h68, as the most attenuated Vaccinia virus strain among the three virus strains

tested, had the lowest virus yield, with only 0.2 and 1.17 viral particles per cell at 72 hours post-infection in BHSD0022 and BHSD0021 hADSCs, respectively. The maximum virus yield was reached in hADSCs infected with GLV-2b372, with 4.97 and 15.4 viral particles per cell at 72 hours post-infection in BHSD0022 and BHSD0021 hADSCs, respectively.

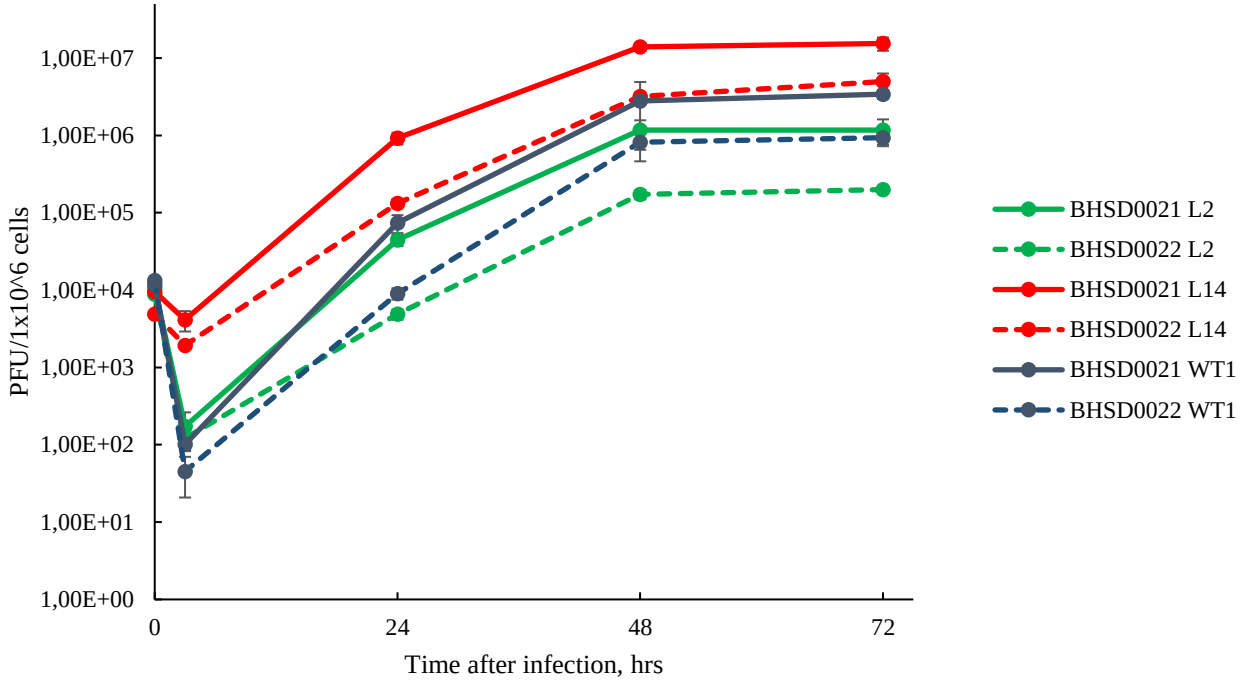

Fig. 20. Viral replication assay of BHSD0021 and BBHSD0022 hADSCs infected with GL-1h68 (L2), GLV-2b372 (L14) and ACAM2000 (WT1) at MOI of 0.01. The cells were grown in 6-well plates to the confluence of 95% and infected with the virus in triplicates. The cells were harvested at 3, 24, 48 and 72 hours post-infection. The virus titers were determined by standard plaque assay according to section 3.2.4. The values are the mean of the triplicates, bars indicate ±SD.

4.2.3. Virus yield is not affected by hADSC passage

ADSCs used in the study could usually be cultured until passages 10-11 when they arrive in quiescence and stop dividing. We analyzed virus production in two hADSC lines from two different donors at different passages and observed no significant virus yield variation between the time points (**Fig. 21**). Through passages 4 to 10, the cells could steadily produce around 10 to 20 effective viral particles, depending on the donor and in a passage-independent manner.

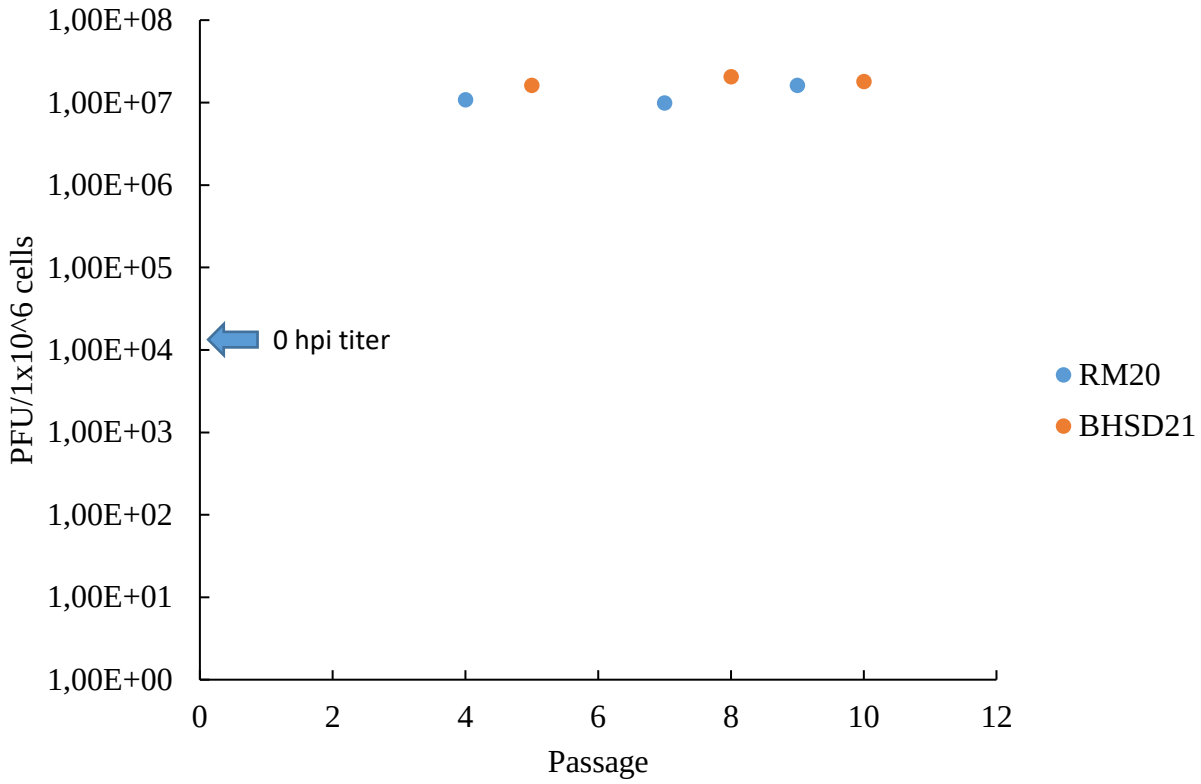

Fig. 21. GLV-2b372 production in hADSCs (RM0020 and BHSD0021) at different cell passages. Blue arrow indicates virus titer at 0 hpi.

4.2.4. ADSC-mediated delivery of Vaccinia virus in athymic xenograft tumor mouse model

We designed a xenograft mouse model to test the ability of infected hADSCs to deliver the virus to the tumor site. A549 xenograft tumor-bearing mice were intravenously treated with either 4x10^5 PFU of LIVP1.1.1-TurboFP635 or with 1x10^5 BHSD0021-GFP hADSCs infected with the virus (at MOI 4 or at MOI 100, which corresponds to 4x10^5 or 1x10^7 PFU/animal). A few mice were treated with the virus or the infected cells intratumorally.

4.2.4.1. Loading VACV into the hADSCs

We decided to use two different MOIs of the virus for infection of hADSCs prior to their administration to the animals. BHSD0021 hADSCs were incubated with LIVP1.1.1-TurboFP635 at MOI 4 and MOI 100 for 1 hour at 37C on a rotating waver shaker, washed to eliminate any residual virus particles that have not entered the cells within 1 hour and 6 hours after infection the percentage of fluorescent cells was examined by FACS. When infected at MOI 4, 78% of the cells were expressing TurboFP635 (**Fig. 22**). At MOI 100, 92% of the cells were TurboFP635-positive.

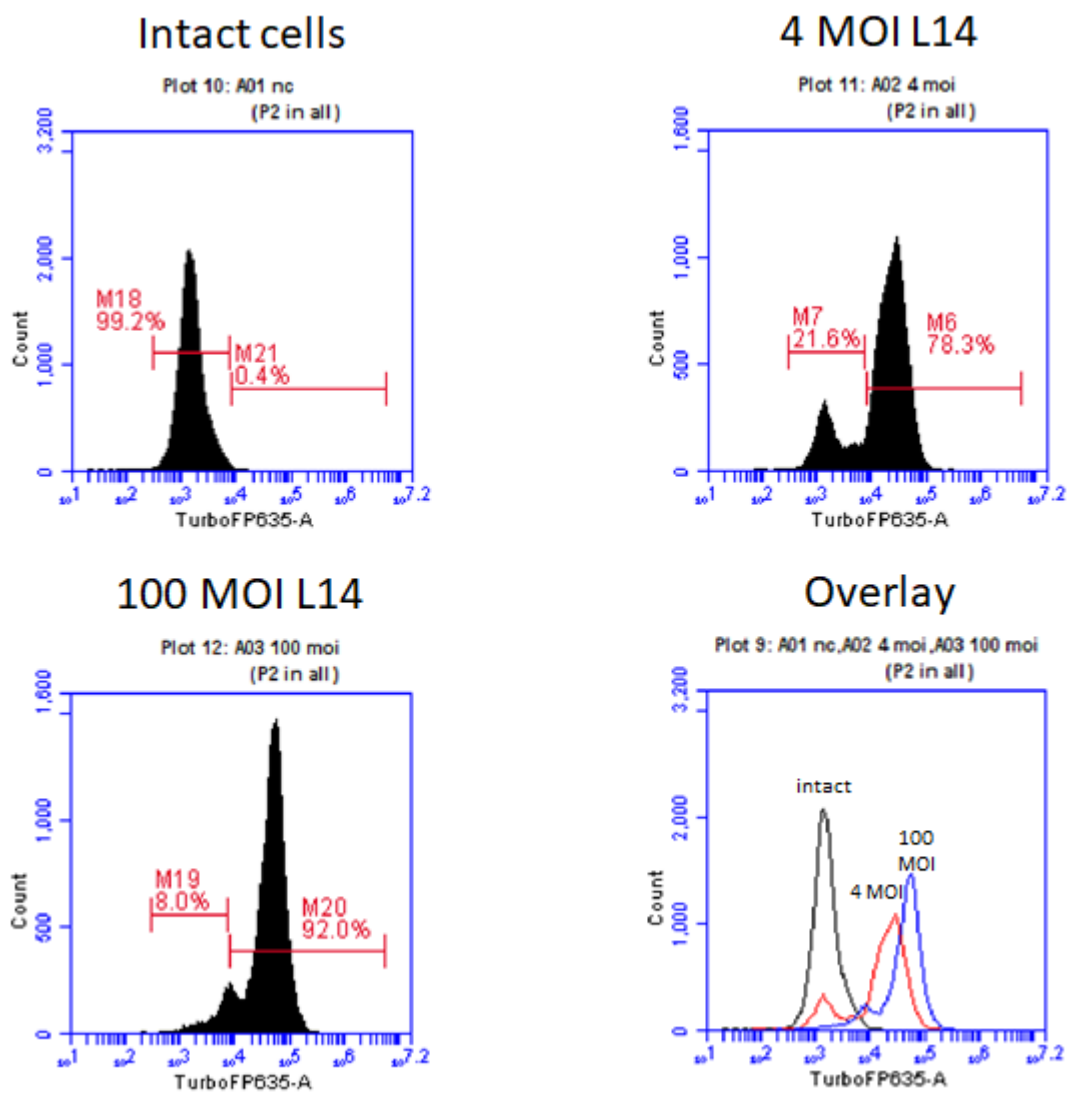

Fig. 22. Turbo-FP635 expression in hADSCs infected with GLV-2b372 after 6 hours post-infection.

4.2.4.2. Viability of hADSCs after infection at 4 and 100 MOIs

We analyzed the viability of BHSD0021 hADSCs at 6 hours after infection with LIVP1.1.1-TurboFP635 virus at MOIs 4 and 100 as described in section 3.2.7. of current work. 94,6% and 94,0% of the cells infected at MOI 4 and infected at MOI 100, respectively, were alive at 6 hours post-infection (**Fig. 23**). For comparison, the viability of non-infected BHSD0021 cells treated otherwise in the same conditions was 98,6%.

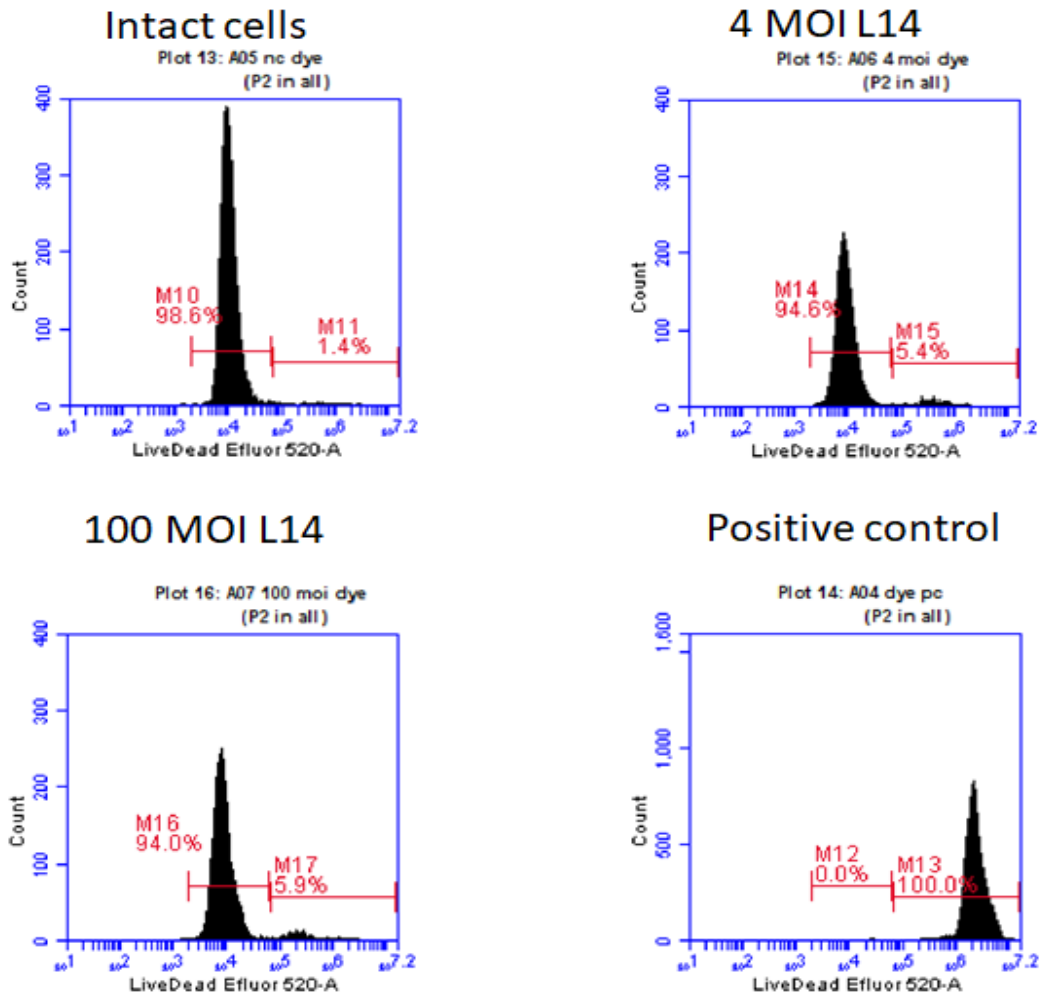

Fig. 23. Viability of hADSCs after 6 hours after infection with GLV-2b372. Dead cells are gated on M11, M15, M17 and M13 gates.

4.2.4.3. Analysis of tumor growth and survival

We observed that treatment with the virus or the virus-infected cells resulted in significant irreversible tumor shrinkage in all treated groups compared to the control group, where the mice were injected with the non-infected hADSCs. hADSC-mediated delivery of the virus resulted in a more rapid tumor regression when compared to the mice treated with the naked virus (**Fig. 24**). When injected intratumorally, no difference in tumor reduction was observed between the group treated with the virus alone and the group treated with the virus-infected hADSCs (**Fig. 25**).

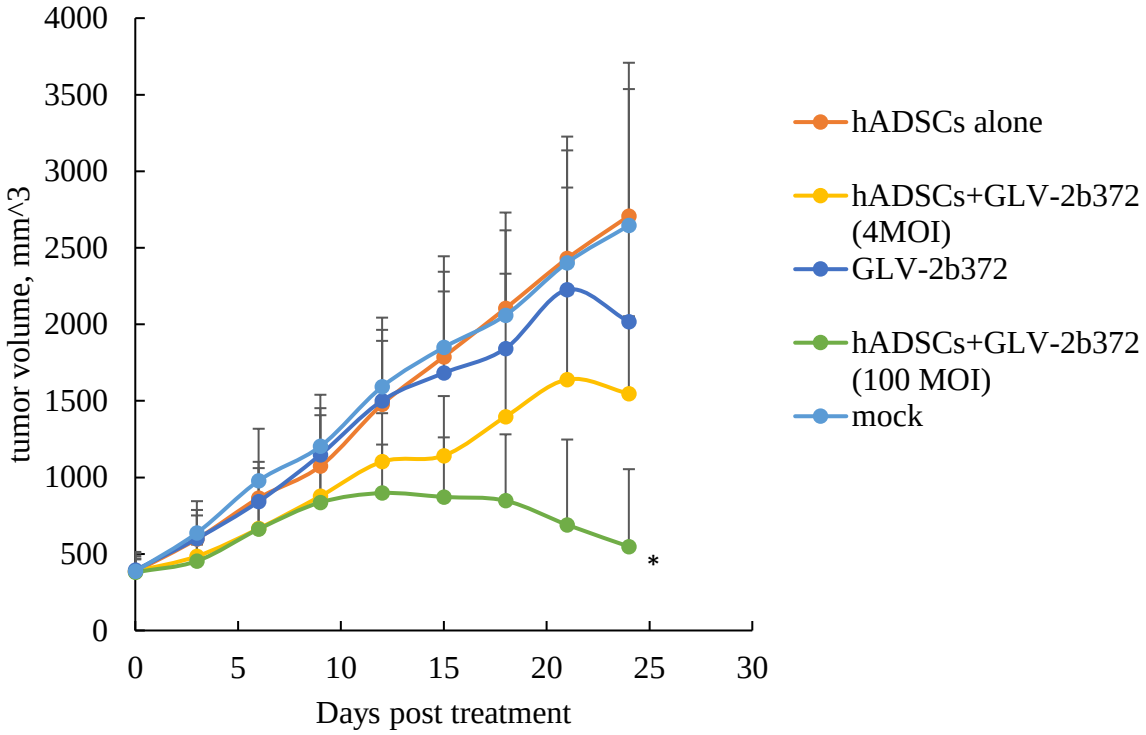

Fig. 24. Tumor growth curves in A549 xenograft animals treated with $1x10^5$ hADSCs loaded with GLV-2b372, intravenous delivery. Naked virus was injected in amount equal to the amount of the virus used for infection of hADSCs at MOI 4. * - statistically significant difference.

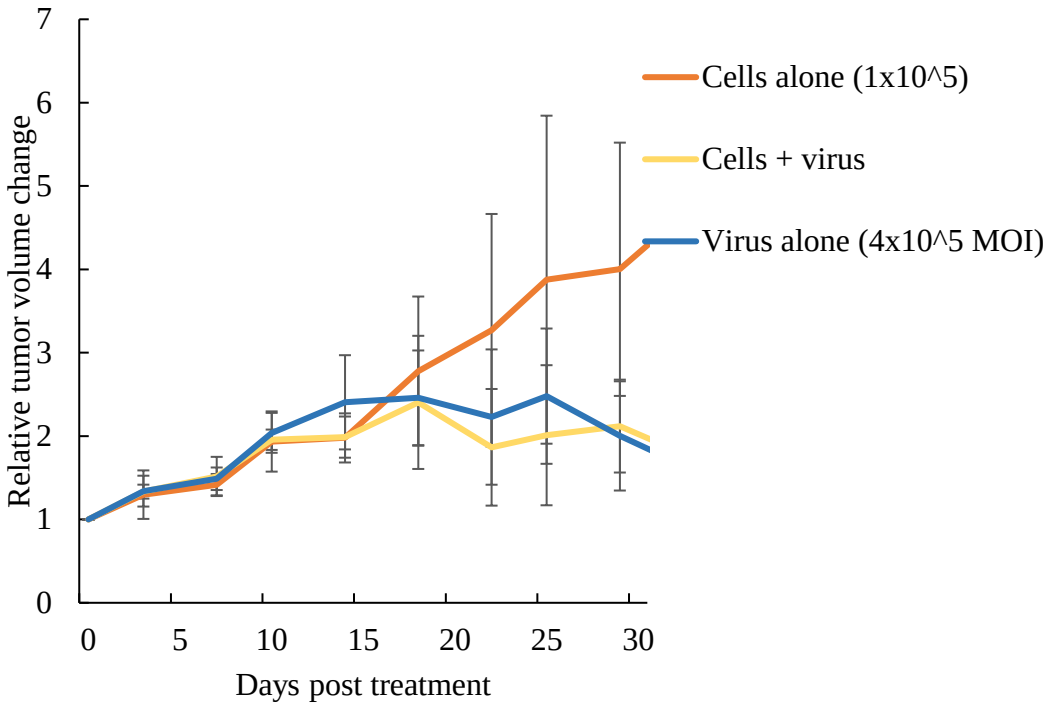

Fig. 25. Tumor growth curves in A549 xenograft animals treated with $1x10^5$ hADSCs loaded with GLV-2b372, intratumoral delivery. Naked virus was injected in amount equal to the amount of the virus used for infection of hADSCs at MOI 4.

4.2.4.4. Analysis of hADSC distribution in treated animals

The distribution of cells in animals injected with hADSCs infected at MOI 4 and non-infected hADSCs was analyzed at 5 and 24 hours post-injection using real-time qPCR as described in section 3.2.8 of Methods. At 5 hours post-injection, non-infected hADSCs were found in kidneys (33,5% of detected cells), liver (24,5%), spleen (11,6%), heart (6,4%), lungs (2,3%) and tumor (21,7%) (**Fig. 26**). At 24 hours after injection the cells were found in heart (31,9% of detected cells), lungs (15,6%), liver (12,7%), kidneys (10,4%), spleen (2,9%) and tumor (26,6%). When infected with GLV-2b372 at MOI 4, the majority of detected cells or their remains at 5 hours post-injection has been found in the liver (89,5%). 5,5% of infected cells have been detected in the

spleen and 5,0% — in kidneys. 24 hours after injection, the majority of the cells or their remains have been still traced in the liver (87,7%), while 10,6% of the cells were found in kidneys and 1,7% — in the spleen.

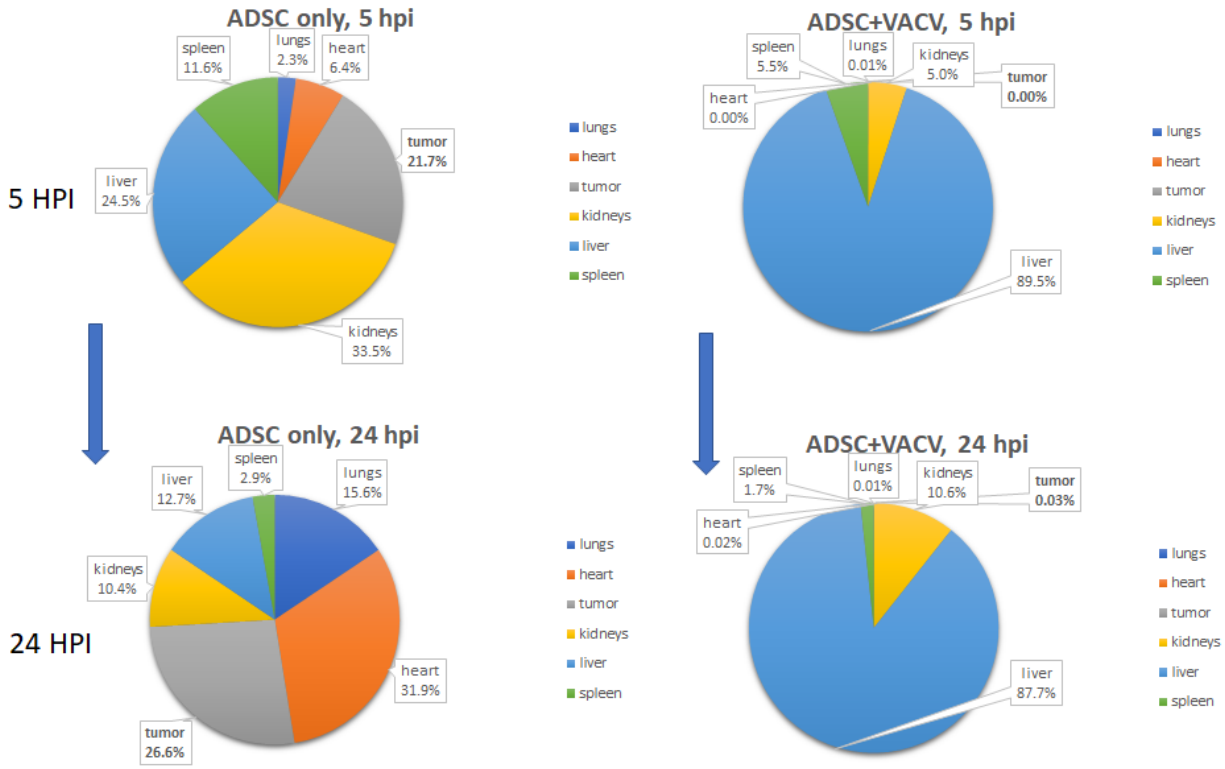

Fig. 26. Distribution of intact hADSCs and hADSCs infected with GLV-2b372 at 5 and 24 hours after intravenous injection.

4.2.9. Analysis of virus distribution in treated animals

The virus spread was analyzed by real-time qPCR as described in section 3.2.8 of Materials and Methods. When injected naked, the majority of the virus DNA can be found in the liver (93,8% of detected viral DNA) at 5 hours post-injection (**Fig. 27**). At 24 hours post-injection, the majority of the virus has been found in tumor (60,7%) and liver (35,8%). When loaded into hADSCs, the virus

distribution is slightly different when compared to the naked virus. At 5 hours after injection, 24,6% of viral DNA is found in the lungs and 71,5% — in the liver. By 24 hours post-infection, most of the virus DNA is again found in the tumor (52,1%) and spleen (32,7%), while a certain proportion of the virus can still be traced in the lungs (13,1%).

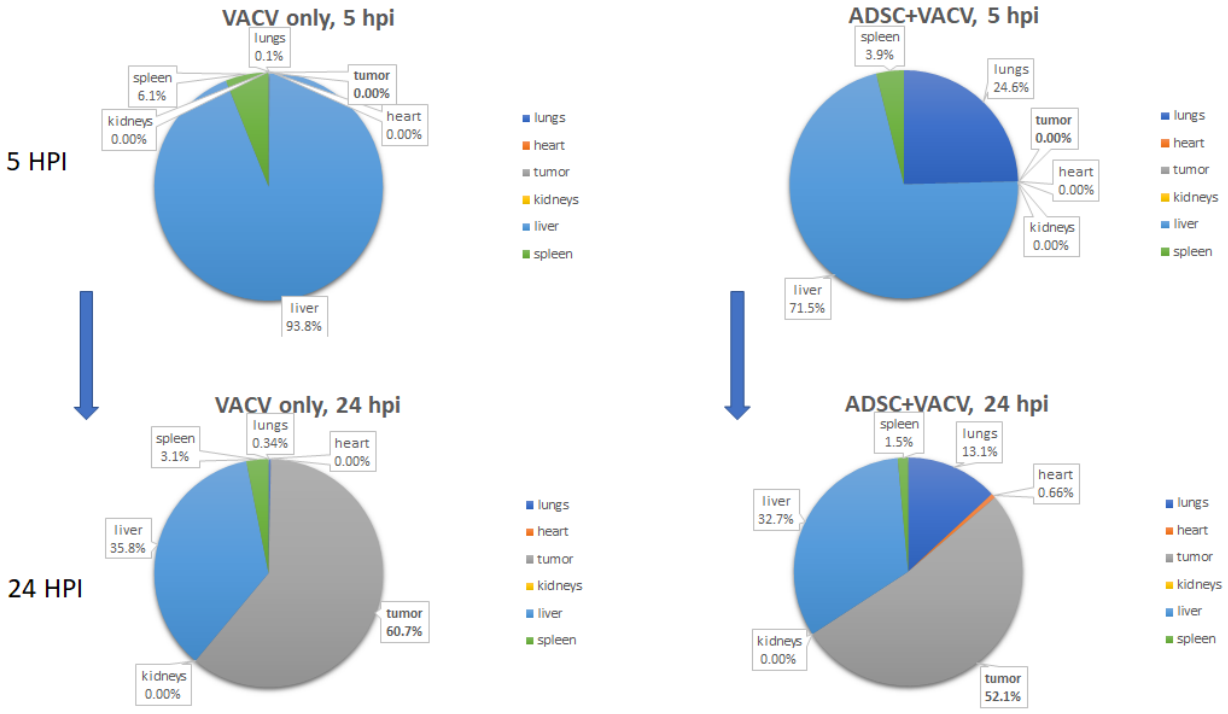

Fig. 27. Distribution of VACV in animals treated with naked GLV-2b372 or with GLV-2b372 loaded into hADSCs at 5 and 24 hours after intravenous injection.

CHAPTER 5: DISCUSSION

5.1. IL-2 armed Vaccinia virus shows oncolytic potential in a syngeneic mouse model

Most of the preclinical data on oncolytic Vaccinia virus is being generated in immunocompromised xenograft murine models, which is understandable due to Vaccinia virus normally not being able to replicate in murine cells. Unfortunately, the xenograft data is sometimes hard to be translated well into clinical use. In the first part of the current study, we attempted to focus on using syngeneic murine cancer models to study cancer therapy with oncolytic Vaccinia virus.

Replication analysis of fourteen different engineered Vaccinia virus strains revealed in 4T1 murine breast carcinoma cells revealed the ability of all the engineered strains to be able to produce new virus progeny in these cells. All of the COP15.1.1 backbone viruses could multiply up to 10 PFU/cell level, depending on the payload (encoded IFNg significantly reduced the ability of the viruses to generate new virus progeny when compared to IL-2 expressing viruses), while LIVP backbone viruses had a very limited ability to replicate in the cells (on average, a 100-fold less LIVP1.1.1 based viruses could be produced in 4T1 cells *in vitro*). Interestingly, when all the tested viruses were applied to the syngeneic 4T1 murine cancer model, treatment with Copenhagen backbone viruses did not result in tumor regression/delay or a survival benefit, while treatment of the tumors with some of the LIVP backbones, especially IL-2 expressing ones, led to a significant tumor growth delay and subsequently extended survival of the animals. At the same time, treatment with IL-2 expressing LIVP1.1.1 viruses was accompanied by short-term treatment-mediated toxicity, which was detected by assessing the weights of the treated animals. The only group where IL-2 blood serum levels were above the detection limit, was the group that had the strongest response to the treatment in terms of tumor growth delay, survival benefit as well as treatment-mediated toxicity, proving that all of the above is caused by the effect of the virus payload.

It is known that in humans, the application of IL-2 has a major side effect, so-called vascular leak syndrome (VLS) that occurs after consistent treatment of patients with high-dose IL-2 treatment [67]. Moreover, it was shown that cancer patients who responded better to the IL-2 treatment also were more susceptible to VLS [99]. In mice, IL-2 causes VLS in the C57Bl/6 inbred strain but not in the BALB/c one [100], probably meaning that we should expect more antitumor effects of IL-2 treatment in C57Bl/6 mice. Therefore, after already quite promising data obtained from 4T1-bearing BALB/c mice, we decided to test the virus in B16F10 melanoma C57Bl/6 mouse model, expecting more therapeutic benefit along with possibly more adverse side effects of the treatment. In that animal study, we also combined the IL-2 expressing virus with either cyclophosphamide (CPA) or romidepsin to study possible synergistic effects of the agents, since there are already multiple reports on synergistic effects of exogenous IL-2 and CPA as well as one of the histone deacetylase inhibitors, MS-275.

In the B16F10 melanoma mouse model, neither treatment with IL-2 expressing Vaccinia virus alone nor in combination with romidepsin did not result in any therapeutic benefit. The combination of the virus with CPA significantly prolonged the survival of the animals, although tumor growth delay was not statistically significant. At the same time, treatment with the IL-2 virus alone, but not in combination with any of the chemotherapeutic agents, resulted in severe irreversible weight loss of most of the treated animals. Virus distribution analysis showed that the virus preferentially colonized the tumor and virus titers in organs were minimal, meaning that the weight loss was probably associated with IL-2 induced VLS. CPA, as well as romidepsin, mediated the toxicity of the virus, although the mechanism of it was not clear.

5.1.1. Combination of IL-2 Vaccinia virus with cyclophosphamide is not only improving therapeutic efficacy but also reduced overall treatment toxicity

To further analyze the synergistic effect of CPA and IL-2 expressing Vaccinia virus, we designed an animal study in the same B16F10 melanoma model, but with different timings and dosages of CPA application. This time, low and high dosage of CPA was applied either two days before, two days after or on the same day with oncolytic Vaccinia virus administration. Virus distribution, as well as IL-2 and IFNg levels in both blood and tumor site, were assessed on days 4 and 7 after virus administration. All the combination-treated groups showed tumor growth delay when compared to CPA low dose treatment alone. Pretreatment of the animals with high dose of CPA treatment two days before virus administration resulted in remarkable tumor shrinkage and its subsequent growth arrest until the endpoint of the experiment. Interestingly, no virus could be found in the tumors of the mice from the group, although some levels of exogenous IL-2 could be detected in both blood and tumor of the animals. At the same time, the best responder group was also the only one, that quickly gained back the weight after weight loss accompanied by treatment in all combination groups. IFNg was detected in tumors of all groups except for the best responder group, which could explain the tumor growth arrest in the group since it is known that IFNg plays an important role in establishing immunosuppressive tumor microenvironment [94].

5.2. ADSC mediated delivery of Vaccinia virus

It is known that oncolytic viruses and especially Vaccinia virus are susceptible to the host immune system upon administration in the bloodstream. 95% to 99% of virus particles administered intravenously do not reach sites of tumor and end up being eliminated by the host complement system, NK cells and/or neutralizing antibodies. Packaging virus into various vehicles, such as lysosomes or cells, might help the virus evade many immune barriers and reach the tumor more

effectively. That could significantly reduce virus doses used in oncolytic virus therapy, which in turn may result in safer and more cost-effective anticancer therapy.

In our work, we analyzed the feasibility of packaging Vaccinia virus into human ADSCs. The cells are mesenchymal stem cells derived from stromal vascular fraction of fat tissue. Upon many features mesenchymal stem cells possess, they are known for their ability to home inflammation and/or tumor sites. Here, we have shown for the first time, that hADSCs can support productive Vaccinia virus replication and the combination can be effectively used for the treatment of tumors in our animal model.

We demonstrated that hADSCs could be a promising carrier system for oncolytic Vaccinia virus. The cells are easy and relatively cheap to obtain and to culture. For instance, the cost of hADSC expansion is approximately 10-fold lower in comparison to CAR-T cells. hADSCs are able to support productive Vaccinia virus replication, and the virus yield is not passage-dependent. It is important, while in our settings the primary cells could be cultured up to passage 10 to 12 when at that point the cells would become quiescent. From the very beginning of hADSC expansion to the very late passages the virus yield was stable and, depending on the donor or the virus strain, virus production could reach 10 to 20 effective viral particles per cell. In comparison, the virus yield of various human tumor cell lines tested for permissivity in our laboratories could be as low as only a few viral particles per cell or as high as thousands of PFU per cell, depending on the tumor cell line. In the current work, we have tested two murine tumor cell lines and the virus yield in both of them was comparable to the virus yield in human hADSCs.

For more feasible monitoring of the hADSCs both *in vitro* and *in vivo*, we transduced the cells with EF1alpha-eGFP expression vector using 3rd generation lentiviral system. EF1alpha promoter has

been chosen over more classical CMV promoter since the latter might quickly become silenced in the stem cells, at least it has been reported for embryonic stem cells [95].

To test the ability of VACV-loaded hADSCs to deliver the virus to the tumor site, an A549 human lung adenocarcinoma xenograft mouse model study was designed. One hour before i.v. administration, the cells were infected with GLV-2b372 virus at MOI 4 or MOI 100. According to our *in vitro* tests, within 1 hour of incubation with the virus, the virus can infect 78% of the cells incubated with the virus at MOI 4 and 92% of the cells incubated at MOI 100, while keeping ≥94% of cells still alive for at least 6 hours after infection in both cases.

When tested *in vivo*, the Trojan horse concept was safe and efficient, resulting in quick elimination of tumors. Shielding of the virus inside hADSCs resulted in formation of none or close to none pox lesions on the limbs of treated animals, when treatment with the virus alone led to extensive pox formation (data not shown). When injected alone, hADSCs did not affect tumor growth. hADSCs were also tested on whether they can form tumors in the Foxn1nu mice. Subcutaneous implantation of BHSD0021-GFP cells did not result in tumor formation, and the fluorescent signal at the site of implantation was lost within a few days after cell injection (data not shown).

High virus numbers found in the lungs of the animals treated with the Trojan horse concept suggest that hADSCs when injected intravenously are getting trapped in the lungs of the animals, which is in accordance with other researchers findings [96,97]. After a few hours after i.v. administration the cells start to escape from the lungs and at 5 hpi the cells can be found evenly distributed throughout the body, which was also found by other researchers [98]. However, hADSC distribution patterns are drastically different depending on whether the cells are carrying the virus load. Already at 5 hpi most of the hADSCs or, which is more likely, their remains, are found in the liver of treated animals, suggesting that most of the infected cells have been recognized by the

immune system of the host and were eliminated. Analysis of virus distribution together with the tumor regression curves suggests that despite the infected hADSCs being quickly eliminated, the tumor has been successfully colonized by the virus. Rapid tumor regression and lack of common side effects such as pox formation on the limbs and nasal area of the animals shows that even in the immunocompromised animal model, the Trojan horse concept possesses several advantages over treatment with the virus alone.

REFERENCES

1. Ferlay J, Colombet M, Soerjomataram I, Parkin DM, Piñeros M, Znaor A, Bray F. Cancer statistics for the year 2020: An overview. Int J Cancer. 2021 Aug 15;149(4):778–89.

2. Centers for Disease Control and Prevention. An Update on Cancer Deaths in the United States. Atlanta, GA: US Department of Health and Human Services, Centers for Disease Control and Prevention, Division of Cancer Prevention and Control; 2021.

3. Macedo N, Miller DM, Haq R, Kaufman HL. Clinical landscape of oncolytic virus research in 2020. J Immunother Cancer. 2020;8(2).

4. Hanahan D, Weinberg RA. The hallmarks of cancer. Cell. 2000 Jan;100(1):57–70.

5. Hanahan D, Weinberg RA. Hallmarks of cancer: The next generation. Cell. 2011;144(5):646–74.

6. Soto AM, Sonnenschein C. The tissue organization field theory of cancer: a testable replacement for the somatic mutation theory. Bioessays. 2011 May;33(5):332–40.

7. Bizzarri M, Cucina A. SMT and TOFT: Why and How They are Opposite and Incompatible Paradigms. Acta Biotheor. 2016;64(3):221–39.

8. Bedessem B, Ruphy S. SMT or TOFT? How the two main theories of carcinogenesis are made (artificially) incompatible. Acta Biotheor. 2015 Sep;63(3):257–67.

9. Kwasniewski W, Stupak A, Kotarski J, Gozdzicak-Jozefiak A. Chaos and cancers. Theories concerning carcinogenesis. Ginekol Pol. 2021;92(4):318–21.

10. Dales S. The uptake and development of vaccinia virus in strain l cells followed with labeled viral deoxyribonucleic acid. J Cell Biol. 1963 Jul 1;18(1):51–72.

11. Moss B. Poxvirus cell entry: How many proteins does it take? Viruses. 2012;4(5):688–707.

12. Smith GL, Moss B. Infectious poxvirus vectors have capacity for at least 25 000 base pairs of foreign DNA. Gene. 1983;25(1):21–8.

13. Tolonen N, Doglio L, Schleich S, Krijnse Locker J. Vaccinia virus DNA replication occurs in endoplasmic reticulum-enclosed cytoplasmic mini-nuclei. Mol Biol Cell. 2001;12(7):2031–46.

14. Smith GL, Vanderplasschen A, Law M. The formation and function of extracellular enveloped vaccinia virus. J Gen Virol. 2002;83(12):2915–31.

15. Vanderplasschen A, Mathew E, Hollinshead M, Sim RB, Smith GL. Extracellular enveloped vaccinia virus is resistant to complement because of incorporation of host complement control proteins into its envelope. Proc Natl Acad Sci U S A. 1998;95(13):7544–9.

16. Fenner F. The global eradication of smallpox. Med J Aust. 1980;1(10):455–6.

17. Goebel SJ, Johnson GP, Perkus ME, Davis SW, Winslow JP, Paoletti E. The complete DNA sequence of vaccinia virus. Virology. 1990;179(1):247–66.

18. Wyatt LS, Shors ST, Murphy BR, Moss B. Development of a replication-deficient recombinant vaccinia virus vaccine effective against parainfluenza virus 3 infection in an animal model. Vaccine. 1996;14(15):1451–8.

19. Cochran MA, Puckett C, Moss B. In vitro mutagenesis of the promoter region for a vaccinia virus gene: evidence for tandem early and late regulatory signals. J Virol. 1985;54(1):30–7.

20. Moss B, Salzman NP. Sequential Protein Synthesis Following Vaccinia Virus Infection. J Virol. 1968;2(10):1016–27.

21. Vos JC, Stunnenberg HG. Derepression of a novel class of vaccinia virus genes upon DNA replication. EMBO J. 1988 Nov;7(11):3487–92.

22. Bengali Z, Satheshkumar PS, Moss B. Orthopoxvirus species and strain differences in cell entry. Virology. 2012 Nov;433(2):506–12.

23. Schmidt FI, Bleck CKE, Helenius A, Mercer J. Vaccinia extracellular virions enter cells by macropinocytosis and acid-activated membrane rupture. EMBO J [Internet]. 2011;30(17):3647–61. Available from: http://dx.doi.org/10.1038/emboj.2011.245

24. Townsley AC, Weisberg AS, Wagenaar TR, Moss B. Vaccinia Virus Entry into Cells via a Low-pH-Dependent Endosomal Pathway. J Virol. 2006;80(18):8899–908.

25. Mercer J, Knébel S, Schmidt FI, Crouse J, Burkard C, Helenius A. Vaccinia virus strains use distinct forms of macropinocytosis for host-cell entry. Proc Natl Acad Sci U S A. 2010;107(20):9346–51.

26. Carter GC, Rodger G, Murphy BJ, Law M, Krauss O, Hollinshead M, Smith GL. Vaccinia virus cores are transported on microtubules. J Gen Virol. 2003 Sep;84(Pt 9):2443–58.

27. CAIRNS J. The initiation of vaccinia infection. Virology. 1960 Jul;11:603–23.

28. Tomley FM, Cooper RJ. The DNA polymerase activity of vaccinia virus "virosomes": Solubilization and properties. J Gen Virol. 1984;65(4):825–9.

29. Moss B. Origin of the poxviral membrane: A 50-year-old riddle. PLoS Pathog. 2018;14(6):1–6.

30. Sivan G, Weisberg AS, Americo JL, Moss B. Retrograde Transport from Early Endosomes to the trans-Golgi Network Enables Membrane Wrapping and Egress of Vaccinia Virus

Virions. J Virol. 2016 Oct;90(19):8891–905.

31. Boulanger D, Smith T, Skinner MA. Morphogenesis and release of fowlpox virus. J Gen Virol. 2000;81(3):675–87.

32. Laliberte JP, Moss B. Lipid membranes in poxvirus replication. Viruses. 2010;2(4):972–86.

33. Kucerova P, Cervinkova M. Spontaneous regression of tumour and the role of microbial infection--possibilities for cancer treatment. Anticancer Drugs. 2016 Apr;27(4):269–77.

34. Jessy T. Immunity over inability: The spontaneous regression of cancer. J Nat Sci Biol Med. 2011 Jan;2(1):43–9.

35. Jackson R. Saint Peregrine, O.S.M.--the patron saint of cancer patients. Can Med Assoc J. 1974 Oct;111(8):824,827.

36. Hoption Cann SA, van Netten JP, van Netten C. Dr William Coley and tumour regression: a place in history or in the future. Postgrad Med J. 2003 Dec;79(938):672–80.

37. Coley WB. The treatment of malignant tumors by repeated inoculations of erysipelas. With a report of ten original cases. 1893. Clin Orthop Relat Res. 1991 Jan;(262):3–11.

38. Coley WB. The Treatment of Inoperable Sarcoma by Bacterial Toxins (the Mixed Toxins of the Streptococcus erysipelas and the Bacillus prodigiosus). Proc R Soc Med. 1910;3(Surg Sect):1–48.

39. Iwanowski D. Concerning the mosaic disease of the tobacco plant. St. Petersb. Acad.Imp. Sci. Bul. 35: 67-70. Translation published in English as Phytopathological Classics Number 7 (1942). American Phytopathological Society Press. 1892.

40. Dock G, Company LB&. The Influence of Complicating Diseases Upon Leukaemia Lea

Brothers & Company; 1904.

41. Bierman HR, Crile DM, Dod KS, Kelly KH, Petrakis NL, White LP, Shimkin MB. Remissions in leukemia of childhood following acute infectious disease: staphylococcus and streptococcus, varicella, and feline panleukopenia. Cancer. 1953 May;6(3):591–605.

42. N DP. Sulla scomparsa di un enorme cancro vegetante del collo dell'utero senza cura chirurgica. [On the demise of the a huge vegetating cervical cancer without surgical care]. Ginecologia. 1912;9:82–9.

43. Tayeb S, Zakay-Rones Z, Panet A. Therapeutic potential of oncolytic Newcastle disease virus: a critical review. Oncolytic virotherapy. 2015;4:49–62.

44. Southam CM. Division of microbiology: present status of oncolytic virus studies. Trans N Y Acad Sci. 1960;22(8 Series II):657–73.

45. Levaditi C, Nicolau S. Sur le culture du virus vaccinal dans les neoplasmes epithelieux. CR Soc Biol. 1922;(86):928.

46. Kelly E, Russell SJ. History of oncolytic viruses: genesis to genetic engineering. Mol Ther. 2007 Apr;15(4):651–9.

47. McCart JA, Ward JM, Lee J, Hu Y, Alexander HR, Libutti SK, Moss B, Bartlett DL. Systemic Cancer Therapy with a Tumor-selective Vaccinia Virus Mutant Lacking Thymidine Kinase and Vaccinia Growth Factor Genes. Cancer Res [Internet]. 2001 Dec 15;61(24):8751 LP-8757.

48. Kohn S, Nagy JA, Dvorak HF, Dvorak AM. Pathways of macromolecular tracer transport across venules and small veins. Structural basis for the hyperpermeability of tumor blood vessels. Lab Invest. 1992 Nov;67(5):596–607.

49. Noser JA, Mael AA, Sakuma R, Ohmine S, Marcato P, Lee PW, Ikeda Y. The RAS/Raf1/MEK/ERK signaling pathway facilitates VSV-mediated oncolysis: implication for the defective interferon response in cancer cells. Mol Ther. 2007 Aug;15(8):1531–6.

50. Wojton J, Kaur B. Impact of tumor microenvironment on oncolytic viral therapy. Cytokine Growth Factor Rev. 2010;21(2–3):127–34.

51. Matveeva O V, Chumakov PM. Defects in interferon pathways as potential biomarkers of sensitivity to oncolytic viruses. Rev Med Virol. 2018 Nov;28(6):e2008.

52. Bai Y, Hui P, Du X, Su X. Updates to the antitumor mechanism of oncolytic virus. Thorac cancer. 2019 May;10(5):1031–5.

53. Boucher Y, Jain RK. Microvascular pressure is the principal driving force for interstitial hypertension in solid tumors: implications for vascular collapse. Cancer Res. 1992 Sep;52(18):5110–4.

54. Jain RK, Stylianopoulos T. Delivering nanomedicine to solid tumors. Nat Rev Clin Oncol. 2010 Nov;7(11):653–64.

55. Oh E, Hong J, Kwon O-J, Yun C-O. A hypoxia- and telomerase-responsive oncolytic adenovirus expressing secretable trimeric TRAIL triggers tumour-specific apoptosis and promotes viral dispersion in TRAIL-resistant glioblastoma. Sci Rep. 2018 Jan;8(1):1420.

56. Pipiya T, Sauthoff H, Huang YQ, Chang B, Cheng J, Heitner S, Chen S, Rom WN, Hay JG. Hypoxia reduces adenoviral replication in cancer cells by downregulation of viral protein expression. Gene Ther. 2005 Jun;12(11):911–7.

57. Sheng Guo Z. The impact of hypoxia on oncolytic virotherapy. Virus Adapt Treat. 2011;3(1):71–82.

58. Sharp DW, Lattime EC. Recombinant Poxvirus and the Tumor Microenvironment: Oncolysis, Immune Regulation and Immunization. Biomedicines. 2016;4(3).

59. Marelli G, Howells A, Lemoine NR, Wang Y. Oncolytic Viral Therapy and the Immune System: A Double-Edged Sword Against Cancer. Front Immunol. 2018;9:866.

60. Hernandez-Alcoceba R, Pihalja M, Qian D, Clarke MF. New oncolytic adenoviruses with hypoxia- and estrogen receptor-regulated replication. Hum Gene Ther. 2002 Sep;13(14):1737–50.

61. Schäfer S, Weibel S, Donat U, Zhang Q, Aguilar RJ, Chen NG, Szalay AA. Vaccinia virus-mediated intra-tumoral expression of matrix metalloproteinase 9 enhances oncolysis of PC-3 xenograft tumors. BMC Cancer. 2012 Aug;12:366.

62. Mok W, Boucher Y, Jain RK. Matrix metalloproteinases-1 and -8 improve the distribution and efficacy of an oncolytic virus. Cancer Res. 2007;67(22):10664–8.

63. Ganesh S, Gonzalez-Edick M, Gibbons D, Van Roey M, Jooss K. Intratumoral coadministration of hyaluronidase enzyme and oncolytic adenoviruses enhances virus potency in metastatic tumor models. Clin Cancer Res. 2008;14(12):3933–41.

64. Kuriyama N, Kuriyama H, Julin CM, Lamborn K, Israel MA. Pretreatment with Protease Is a Useful Experimental Strategy for Enhancing Adenovirus-Mediated Cancer Gene Therapy. Hum Gene Ther. 2000;11(16):2219–30.

65. Nagano S, Perentes JY, Jain RK, Boucher Y. Cancer cell death enhances the penetration and efficacy of oncolytic herpes simplex virus in tumors. Cancer Res. 2008 May;68(10):3795–802.

66. Liu BL, Robinson M, Han Z-Q, Branston RH, English C, Reay P, McGrath Y, Thomas SK,

Thornton M, Bullock P, Love CA, Coffin RS. ICP34.5 deleted herpes simplex virus with enhanced oncolytic, immune stimulating, and anti-tumour properties. Gene Ther [Internet]. 2003;10(4):292–303. Available from: https://doi.org/10.1038/sj.gt.3301885

67. Rosenberg SA, Lotze MT. Cancer immunotherapy using interleukin-2 and interleukin-2-activated lymphocytes. Annu Rev Immunol. 1986;4:681–709.

68. Rosenberg SA. IL-2: the first effective immunotherapy for human cancer. J Immunol. 2014 Jun;192(12):5451–8.

69. Acres B, Dott K, Stefani L, Kieny MP. Directed cytokine expression in tumour cells in vivo using recombinant vaccinia virus. Ther Immunol. 1994 Jan;1(1):17–23.

70. Bourgeois-Daigneault M-C, Roy DG, Falls T, Twumasi-Boateng K, St-Germain LE, Marguerie M, Garcia V, Selman M, Jennings VA, Pettigrew J, Amos S, Diallo J-S, Nelson B, Bell JC. Oncolytic vesicular stomatitis virus expressing interferon-σ has enhanced therapeutic activity. Mol Ther - Oncolytics. 2016;3:16001.

71. Kober C, Weibel S, Rohn S, Kirscher L, Szalay AA. Intratumoral INF-γ triggers an antiviral state in GL261 tumor cells: a major hurdle to overcome for oncolytic vaccinia virus therapy of cancer. Mol Ther oncolytics. 2015;2:15009.

72. Raykov Z, Rommelaere J. Potential of tumour cells for delivering oncolytic viruses. Gene Ther . 2008;15(10):704–10.

73. Roberts DM, Nanda A, Havenga MJE, Abbink P, Lynch DM, Ewald BA, Liu J, Thorner AR, Swanson PE, Gorgone DA, Lifton MA, Lemckert AAC, Holterman L, Chen B, Dilraj A, Carville A, Mansfield KG, Goudsmit J, Barouch DH. Hexon-chimaeric adenovirus serotype 5 vectors circumvent pre-existing anti-vector immunity. Nature.

2006;441(7090):239–43.

74. Thirunavukarasu P, Sathaiah M, Gorry MC, O'Malley ME, Ravindranathan R, Austin F, Thorne SH, Guo ZS, Bartlett DL. A rationally designed A34R mutant oncolytic poxvirus: improved efficacy in peritoneal carcinomatosis. Mol Ther. 2013 May;21(5):1024–33.

75. VanSeggelen H, Tantalo DGM, Afsahi A, Hammill JA, Bramson JL. Chimeric antigen receptor–engineered T cells as oncolytic virus carriers. Mol Ther - Oncolytics. 2015;2:15014.

76. Shin DH, Nguyen T, Ozpolat B, Lang F, Alonso M, Gomez-Manzano C, Fueyo J. Current strategies to circumvent the antiviral immunity to optimize cancer virotherapy. J Immunother Cancer. 2021;9(4).

77. Patel MR, Dash A, Jacobson BA, Ji Y, Baumann D, Ismail K, Kratzke RA. JAK/STAT inhibition with ruxolitinib enhances oncolytic virotherapy in non-small cell lung cancer models. Cancer Gene Ther. 2019 Nov;26(11–12):411–8.

78. Nusinzon I, Horvath CM. Interferon-stimulated transcription and innate antiviral immunity require deacetylase activity and histone deacetylase 1. Proc Natl Acad Sci U S A. 2003 Dec;100(25):14742–7.

79. Marchini A, Scott EM, Rommelaere J. Overcoming Barriers in Oncolytic Virotherapy with HDAC Inhibitors and Immune Checkpoint Blockade. Viruses. 2016 Jan;8(1).

80. MacTavish H, Diallo J-S, Huang B, Stanford M, Le Boeuf F, De Silva N, Cox J, Simmons JG, Guimond T, Falls T, McCart JA, Atkins H, Breitbach C, Kirn D, Thorne S, Bell JC. Enhancement of vaccinia virus based oncolysis with histone deacetylase inhibitors. PLoS One. 2010 Dec;5(12):e14462.

81. Merluzzi VJ, Walker MM, Faanes RB. Inhibition of cytotoxic T-cell clonal expansion by cyclophosphamide and the recovery of cytotoxic T-lymphocyte precursors by supernatants from mixed-lymphocyte cultures. Cancer Res. 1981 Mar;41(3):850–3.

82. Hofmann E, Weibel S, Szalay AA. Combination treatment with oncolytic Vaccinia virus and cyclophosphamide results in synergistic antitumor effects in human lung adenocarcinoma bearing mice. J Transl Med. 2014 Jul;12:197.

83. Mader EK, Maeyama Y, Lin Y, Butler GW, Russell HM, Galanis E, Russell SJ, Dietz AB, Peng K-W. Mesenchymal Stem Cell Carriers Protect Oncolytic Measles Viruses from Antibody Neutralization in an Orthotopic Ovarian Cancer Therapy Model. Clin Cancer Res . 2009;15(23):7246–55.

84. Smith CL, Chaichana KL, Lee YM, Lin B, Stanko KM, O'Donnell T, Gupta S, Shah SR, Wang J, Wijesekera O, Delannoy M, Levchenko A, Quiñones-Hinojosa A. Pre-Exposure of Human Adipose Mesenchymal Stem Cells to Soluble Factors Enhances Their Homing to Brain Cancer. Stem Cells Transl Med. 2015;4(3):239–51.

85. Xie C, Yang Z, Suo Y, Chen Q, Wei D, Weng X, Gu Z, Wei X. Systemically Infused Mesenchymal Stem Cells Show Different Homing Profiles in Healthy and Tumor Mouse Models. Stem Cells Transl Med . 2017;6(4):1120–31.

86. Hadryś A, Sochanik A, McFadden G, Jazowiecka-Rakus J. Mesenchymal stem cells as carriers for systemic delivery of oncolytic viruses. Eur J Pharmacol. 2020;874:172991.

87. Lin W, Huang L, Li Y, Fang B, Li G, Chen L, Xu L. Mesenchymal Stem Cells and Cancer: Clinical Challenges and Opportunities. Biomed Res Int. 2019;2019:2820853.

88. Zhong W, Tong Y, Li Y, Yuan J, Hu S, Hu T, Song G. Mesenchymal stem cells in

inflammatory microenvironment potently promote metastatic growth of cholangiocarcinoma via activating Akt/NF-κB signaling by paracrine CCL5. Oncotarget. 2017 Sep;8(43):73693–704.

89. Ho IAW, Toh HC, Ng WH, Teo YL, Guo CM, Hui KM, Lam PYP. Human bone marrow-derived mesenchymal stem cells suppress human glioma growth through inhibition of angiogenesis. Stem Cells. 2013 Jan;31(1):146–55.

90. Yulyana Y, Ho IAW, Sia KC, Newman JP, Toh XY, Endaya BB, Chan JKY, Gnecchi M, Huynh H, Chung AYF, Lim KH, Leong HS, Iyer NG, Hui KM, Lam PYP. Paracrine Factors of Human Fetal MSCs Inhibit Liver Cancer Growth Through Reduced Activation of IGF-1R/PI3K/Akt Signaling. Mol Ther. 2015 Apr 1;23(4):746–56.

91. Zhang Q, Yu YA, Wang E, Chen N, Danner RL, Munson PJ, Marincola FM, Szalay AA. Eradication of solid human breast tumors in nude mice with an intravenously injected light-emitting oncolytic vaccinia virus. Cancer Res. 2007 Oct;67(20):10038–46.

92. Tsoneva D, Minev B, Frentzen A, Zhang Q, Wege AK, Szalay AA. Humanized Mice with Subcutaneous Human Solid Tumors for Immune Response Analysis of Vaccinia Virus-Mediated Oncolysis. Mol Ther oncolytics. 2017 Jun;5:41–61.

93. Mosmann T. Rapid colorimetric assay for cellular growth and survival: Application to proliferation and cytotoxicity assays. J Immunol Methods. 1983;65(1):55–63.

94. Mojic M, Takeda K, Hayakawa Y. The Dark Side of IFN-γ: Its Role in Promoting Cancer Immunoevasion. Int J Mol Sci. 2017 Dec;19(1).

95. Norrman K, Fischer Y, Bonnamy B, Wolfhagen Sand F, Ravassard P, Semb H. Quantitative comparison of constitutive promoters in human ES cells. PLoS One. 2010 Aug;5(8):e12413.

96. Eggenhofer E, Benseler V, Kroemer A, Popp F, Geissler E, Schlitt H, Baan C, Dahlke M, Hoogduijn M. Mesenchymal stem cells are short-lived and do not migrate beyond the lungs after intravenous infusion. Front Immunol. 2012;3.

97. Saat TC, van den Engel S, Bijman-Lachger W, Korevaar SS, Hoogduijn MJ, IJzermans JNM, de Bruin RWF. Fate and Effect of Intravenously Infused Mesenchymal Stem Cells in a Mouse Model of Hepatic Ischemia Reperfusion Injury and Resection. Bussolati B, editor. Stem Cells Int. 2016;2016:5761487.

98. Boddington S, Henning TD, Sutton EJ, Daldrup-Link HE. Labeling stem cells with fluorescent dyes for non-invasive detection with optical imaging. J Vis Exp. 2008 Apr;(14).

99. Rosenberg SA, Lotze MT, Yang JC, Aebersold PM, Linehan WM, Seipp CA, White DE. Experience with the use of high-dose interleukin-2 in the treatment of 652 cancer patients. Ann Surg. 1989 Oct;210(4):474–5.

100. Melencio L, McKallip RJ, Guan H, Ramakrishnan R, Jain R, Nagarkatti PS, Nagarkatti M. Role of CD4(+)CD25(+) T regulatory cells in IL-2-induced vascular leak. Int Immunol. 2006 Oct;18(10):1461–71.

ACKNOWLEDGMENTS

Current work was carried out in Genelux Corp, San Diego, CA, USA, and at the Department of Biochemistry, the University of Wuerzburg, Bavaria, Germany. The research was supported by research and a service grant from Genelux Corporation (R&D facility in San Diego, CA, USA), DFG, StemImmune Inc, and by Hope Realized Medical Foundation. I.P. was a recipient of a graduate fellowship from research grants awarded to AA Szalay.

I would like to thank Genelux Corp, CA, USA, and the University of Wuerzburg for providing me the opportunity to work on and complete my Ph.D. program.

I would especially thank my supervisor, Prof. Dr. Szalay, for always supporting me and never giving up on me during my Ph.D. research.

I am grateful to all employees of Genelux Corp I worked with during my internship in their facilities, especially I would like to thank Jochen Strizker, Nanhai Chen, Alexa Frenzen, and Jason Aguilar for their technical assistance and intellectual input.

I would like to mention my former colleagues at StemImmune Inc, Dobrin Draganov, Antonio Santidrian, Boris Minev, and Alex Kilinc for helping me with the animal experiments and discussing with me our preclinical studies.

I am thankful to all my former colleagues at the Department of Biochemistry, especially Ivaylo Gentschev, Barbara Haertl. Cristina Kober, Lorenz Kircher, Dominik Bohn, Sasha Huppertz, Anna Vyalkova and Mingyu Ye.

Last but not least, I would like to thank my family for always supporting me during all these years living away from home in foreign countries.

LIST OF ABBREVIATIONS

◦C	Degrees Celsius
µg	Microgram
µl	Microlitre
AB	Antibodies
ATCC	American Type Culture Collection
CMC	Carboxymethylcellulose
CO_2	Carbon dioxide
DMEM	Dubelcco’s Modified Eagle's Medium
DMSO	Dimethyl sulfoxide
DNA	Deoxyribonucleic Acid
dpi	Days post virus injection/infection
EtOH	Ethanol
FBS	Fetal Bovine Serum
g	Grams
h	Hour
hADSC	Human Adipose-Derived Stem Cells
hpi	Hours post-infection
kbp	Kilobase pairs
LIVP	Lister vaccine strain
mg	Milligram
min	Minute
ml	Millilitre
mm	Millimeter
mM	Millimolar
MOI	Multiplicity of Infection
MTT	Dimethyl thiazolyl diphenyl tetrazolium salt
ng	Nanogram
nm	Nanometre
PBS	Phosphate-Buffered Saline
PFA	Paraformaldehyde

PFU	Plaque Forming Units
r.t.	Room temperature
rpm	Revolutions per minute
SD	Standard Deviation
TurboFP635	Far-Red Fluorescent Protein
U/ml	Units/millilitre
VACV	Vaccinia Virus
VEGF	Vascular Endothelial Growth Factor
VPA	Viral Production Assay
VPA	Viral Production Assay
WHO	World Health Organization

PUBLICATION LIST AND CONFERENCE CONTRIBUTION

1) Gentschev I, Patil SS, Petrov I, Cappello J, Adelfinger M, Szalay AA. Oncolytic virotherapy of canine and feline cancer. Viruses. 2014 May 16;6(5):2122-37. doi: 10.3390/v6052122. PMID: 24841386; PMCID: PMC4036544.

2) Draganov DD, Santidrian AF, Minev I, Nguyen D, Kilinc MO, Petrov I, Vyalkova A, Lander E, Berman M, Minev B, Szalay AA. Delivery of oncolytic vaccinia virus by matched allogeneic stem cells overcomes critical innate and adaptive immune barriers. J Transl Med. 2019 Mar 27;17(1):100. doi: 10.1186/s12967-019-1829-z. Erratum in: J Transl Med. 2021 Oct 4;19(1):414. PMID: 30917829; PMCID: PMC6437877.

3) Petrov I, Gentschev I, Vyalkova A, Elashry MI, Klymiuk MC, Arnhold S, Szalay AA. Canine Adipose-Derived Mesenchymal Stem Cells (cAdMSCs) as a "Trojan Horse" in Vaccinia Virus Mediated Oncolytic Therapy against Canine Soft Tissue Sarcomas. Viruses. 2020 Jul 12;12(7):750. doi: 10.3390/v12070750. PMID: 32664672; PMCID: PMC7411685.

4) Petrov I, Szalay AA. “Combinational therapy of tumors in syngeneic mouse tumor models with Vaccinia virus strains expressing IL-2 and INF-g” Poster 024 at the 12th International Oncolytic Virus Conference, Rochester (MN, USA). 2019 Oct.

5) Vyalkova A, Petrov I, Szalay AA. “Smallpox Vaccines as potential worldwide Cancer Vaccines” Poster 087 at the 12th International Oncolytic Virus Conference, Rochester (MN, USA). 2019 Oct.

AFFIDAVIT

I hereby confirm that my thesis entitled "**Combinational therapy of tumors in syngeneic mouse tumor models with oncolytic Vaccinia virus strains expressing IL-2 and INF-g. Human adipose tissue-derived stem cell mediated delivery of oncolytic Vaccinia virus.**" is the result of my work. I did not receive any help or support from commercial consultants. All sources and/or materials applied are listed and specified in the thesis. Furthermore, I confirm that this has not yet been submitted as part of another examination process neither in identical nor in a similar form.

Wurzburg,

Place, Date Signature

Eidesstattliche Erklärung

Hiermit erkläre ich an Eides statt, die Dissertation " **Kombinationstherapie von Tumoren in syngenen Maus-Tumormodellen mit onkolytischen Vaccinia-Virenstämmen, die IL-2 und INF-g exprimieren. Übertragung von onkolytischen Vaccinia-Viren durch menschliche Fettstammzellen.**" eigenständig, d.h. insbesondere selbständig und ohne Hilfe eines kommerziellen Promotionsberates, angefertigt und keine anderen als die von mir angegebenen Quellen und Hilfsmittle verwendet zu haben. Ich erkläre außedem, dass die Dissertation weder in gleicher noch in ähnlicher Form bereits in einem anderen Prüfungsverfahren vorgelen hat.

Wurzburg,

Ort, Datum Unterschrift